Surface charge control of the Advanced LIGO mirrors using externally introduced ions.

R. Weiss November 30, 2010, June 14, 2011

Abstract: The surface charge on the LIGO mirrors can be neutralized by introducing positive and negative ions in a clean carrier gas. The note describes a system developed to neutralize surface charge densities as large as 10^{-10} coulombs/cm^2 on the mirrors in the BSC chambers. The surface charging occurs primarily by triboelectricity during pumpout or after mirror contact with earthquake stops and is expected to be controllable by occasional neutralization.

Introduction: Surface charge on the dielectric mirrors is a potential source of low frequency displacement noise and has been observed in initial LIGO to cause rotational and translational offsets of the test mass mirrors. The major source of charging in initial LIGO was the occasional rubbing of the mirror surface against an earthquake stop made of VITON. In Enhanced LIGO the surface of the stops was changed to silicon dioxide, the same material as the mirror and its top most coating, to reduce the difference in Fermi energy of the electrons between the mirror and the stop. The amount of charge transfer was greatly reduced. Nevertheless, with the significant improvement in low frequency performance of Advanced LIGO, the possibility of low frequency noise due to time dependent redistribution of the surface charge density remains.

The charging comes primarily from triboelectricity during pumpout and the occasional mirror collision with an earthquake stop. With high power operation in the arm cavities there is also the possibility of photoelectron emission by double photon photoeffect. The expectation is that the charging rate will be small and that it will be adequate, without excessive loss of duty cycle, to occasionally bring a test mass chamber to several torr of ion bearing boil–off nitrogen to discharge the surface. A surface charge density of 10^{-10} coulombs/cm^2 can be discharged in approximately an hour with the ion generator described in this note.

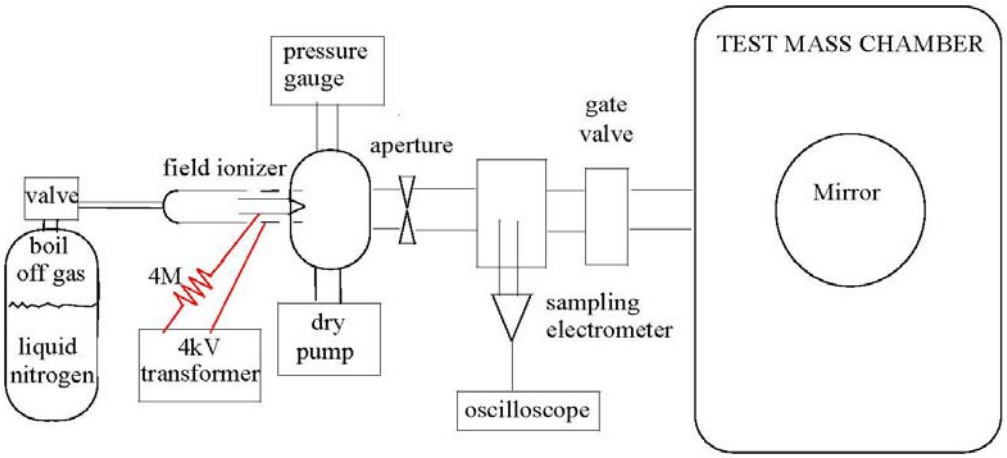

Figure 1 Schematic diagram of the ion generator

Ion generator concept: Figure 1 shows a schematic of the ion generator. Boil off gas from liquid nitrogen is continuously introduced into a region with field ionizing needles driven by 60Hz. As long as the AC voltage is small enough and the nitrogen pressure high enough to avoid initiating a gas discharge (refer to the Paschen curve **Figure 10**), the corona fields at the needles cause the moving nitrogen molecules to ionize, both by losing an electron to make positive ions on the positive half cycle of the 60Hz and to attach electrons on the negative half cycle. The nitrogen pressure between 200 to 500 torr at the needles is maintained by a valve at the input, an aperture into the main tank and by a dry pump. The flow of the neutral gas entraps the ions which head to the 1.5mm apertures that separate the high pressure region at the needles from the low pressure in the test mass chamber. The entrapped ions flow between the electrodes of an electrometer which sample the ion density. The potential of a deflecting electrode near the electrometer collector electrode alternates between positive and negative voltages to extract a few of the ions from the stream to monitor the flow of both positive and negative ions. Finally, the flow passes through a gate valve and into the main chamber where the neutral gas pressure is low enough to allow the ions to freely diffuse and get drawn to the surfaces including the charged surface on the mirror.

The overall strategy of the design is to generate the ions in a region of high pressure where they become entrapped in the neutral gas flow and where there is little chance of a gas discharge. The primary loss of ions in the high pressure flow is through recombination of the positive and negative ions. After the flow has passed the aperture and entered the main chamber, the dominant loss is by diffusion of the ions to the walls.
See the **Appendix 1** for estimates and some of the physics.

The actual apparatus: Figure 2 shows the apparatus as it will be mounted on the BSC chamber to one of the 10 inch conflat flanges at about the height of the mirror.

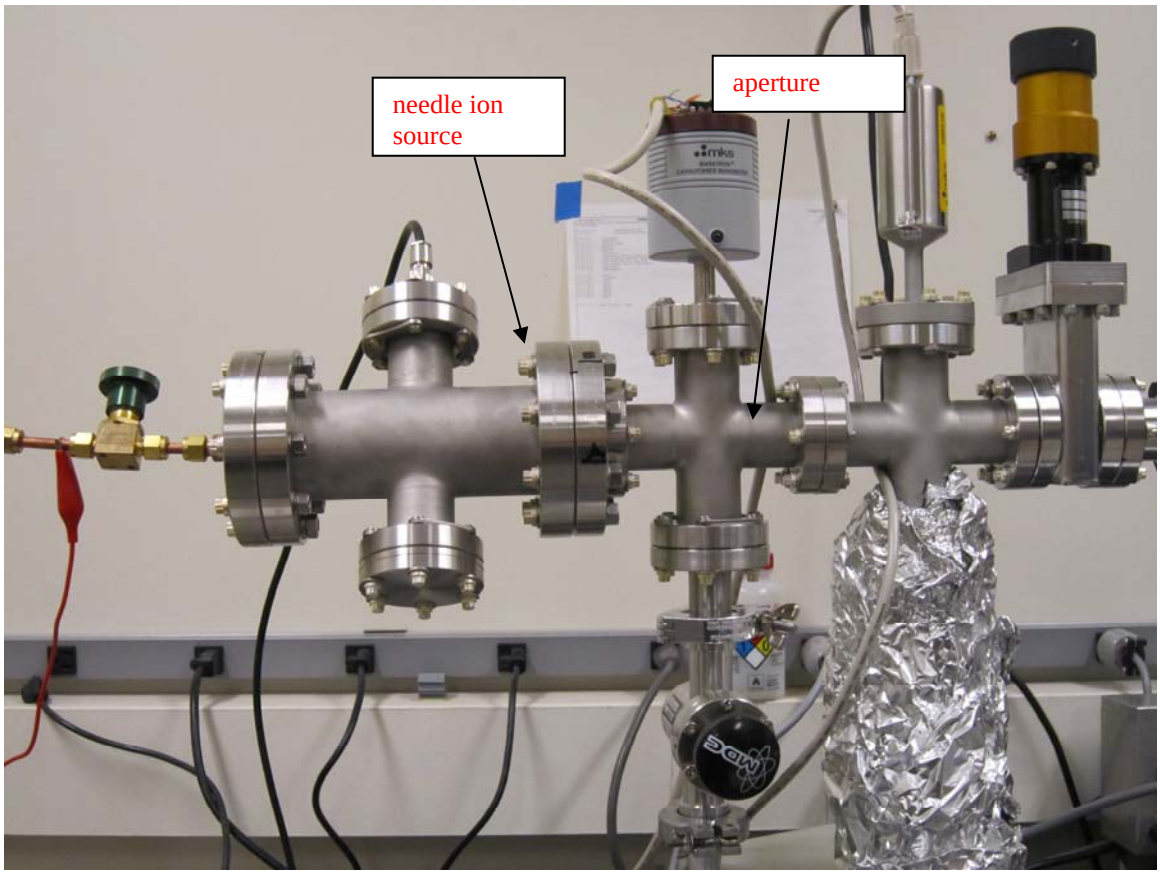

Figure 2 The ion generator to be mounted on a 10 inch conflat "zero" length reducer on one of the 10 inch conflat flanges of a BSC chamber (see **Figure 11**). The nitrogen gas enters the system via the brass NUPRO valve. The needle ion generator (shown in **Figure 3**) is located on the flange on the right of the large cross. A Baratron manometer-pressure gauge measures the pressure between the needle ion generator and the apertures(shown in **Figure 5**). The apertures are mounted in the right flange of the small cross closest to the needles. In much of the operation, the MDC valve to the roughing pump is closed and all the flow is controlled by the NUPRO valve and the flow through the apertures while observing the pressure on the Baratron and the ion yield on the sampling electrometer. The electrometer is mounted at the lower part of the next cross on a multipin header. Several of the wires on the header extend into the flow to sample the ion density. The top of this cross has a Pirani gauge to measure the pressure before opening the gate and NUPRO valves. The gate valve mounts directly on the BSC flange through a short spool piece.

.

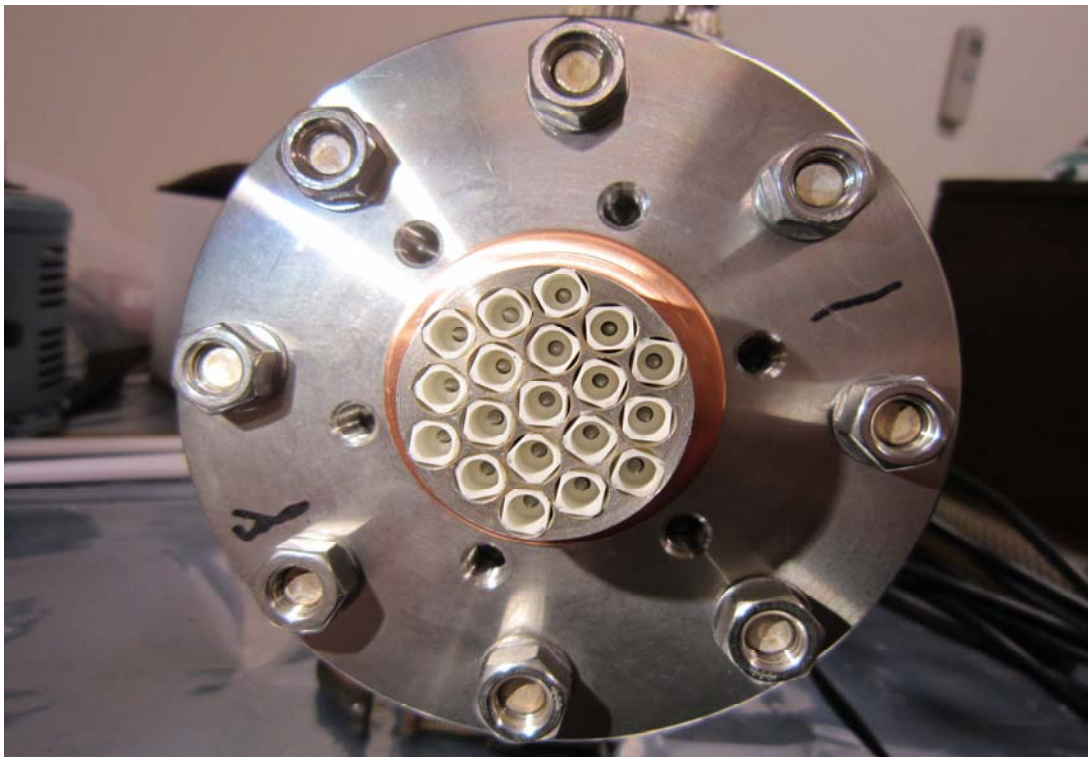

Figure 3 Assembly of 19 needle corona emitters. The gas flows between the square cross section alumina insulators and the round holes in the needle holder block. The ions are formed near the tip of the needle and incorporated in the gas flow Each needle has a 4 megohm resistor in series (shown in **Figure 4**) to limit the current to 1mA rms per needle.

Figure 4 4 Megohm 4 watt Cermet film vacuum compatible resistors manufactured by Dale-Vishay for mercury and sodium vapor lamps. The resistors are fed from a common source and are in series with the individual needles. The resistors can dissipate about 4 watts each when cooled by the nitrogen flow.

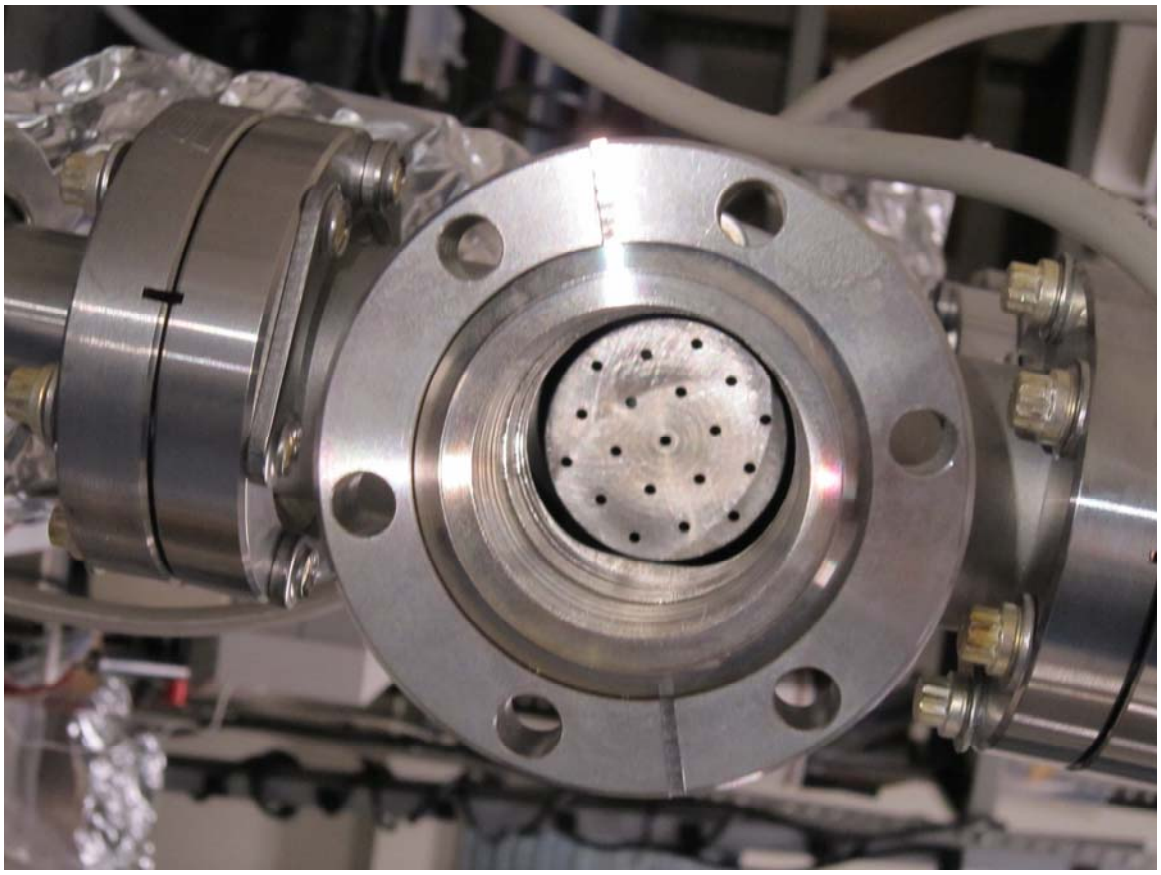

Figure 5 Apertures between the needle ion generator and the main chamber separating the high and low pressure regions of the ion source. The apertures are 1.5 mm in diameter and 3mm long. The maximum ion current flows from the needle sources to the main chamber when the needles and apertures are aligned with each other. One of the final adjustments made in the ion-generator is to maximize the ion signal in the sampling electrometer as the flange holding the needle sources is rotated relative to the aperture plate. The rotation can be made without too large a leak by partially compressing the copper seal in the conflat flange connecting the cross containing the ionizer needles.

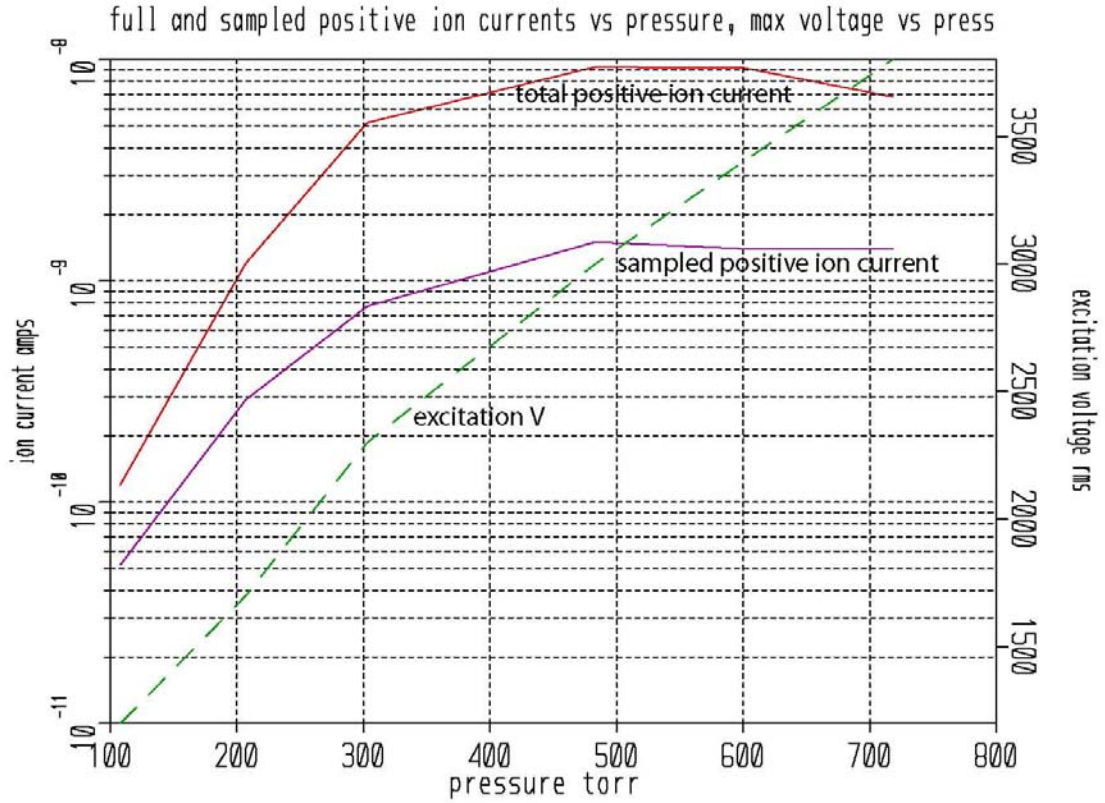

Figure 6 Ion current (left scale) after the aperture and breakdown voltage (right scale) at the needles as a function of pressure. The sampled ion current was measured by the electrometer that is permanently part of the apparatus. The positive and negative ion currents are equal to within 20%. The sampled ion current is about 1/10 of the main ion current flowing into the chamber.

Operation: With the gate valve and the NUPRO valve closed the system is pumped down by the dry pump. The pressure is measured with the Pirani gauge and should come to few millitorr. Next, the NUPRO valve is opened and the system is purged with the nitrogen flowing. The roughing valve is closed and the gate valve is open. The nitrogen pressure in the ionizer is increased to between 200 to 500 torr by adjusting the NUPRO valve. Once the pressure has stabilized, the AC excitation voltage on the ionizer needles is raised (see **Figure 7**) and the AC current flowing between the needles and the vacuum envelope is measured.

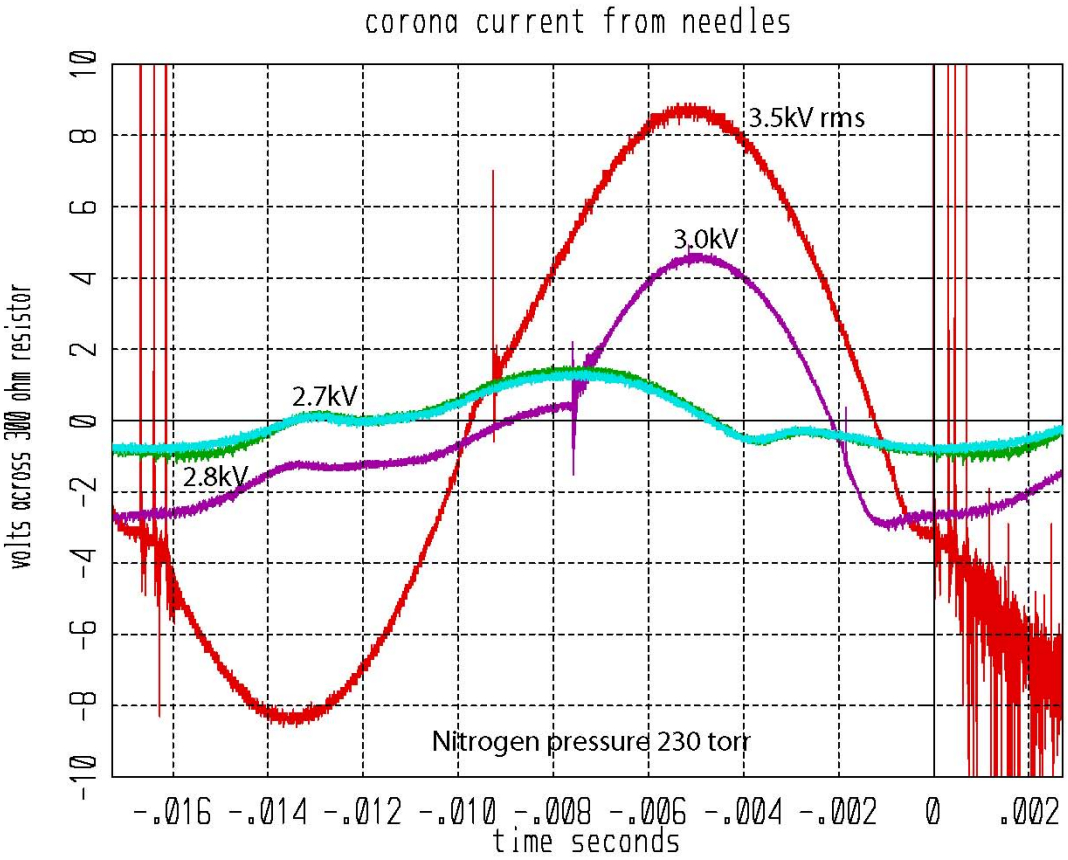

Figure 7 AC current between the needles and ground. With 2.7kV rms the there is no discharge current. At 2.8 kV rms some high frequency structure begins to form at the negative peaks indicating electron emission. At 3kV a discharge oscillation begins to form on several of the needles and , finally, at 3.5kV a full fledged gas discharge occurs at the negative peaks. The positive and negative ion currents are close to equal for excitation voltages less than 2.8kV.

At the same time the sampling electrometer ion current is measured (see **Figure 8**). It is convenient to use a 20 volt peak to peak square wave at 0.1Hz on a deflecting wire in the electrometer to modulate the ion current deflected to the electrometer input wire. The electrometer will collect positive ions for one polarity of the square wave and negative ions with opposite polarity.

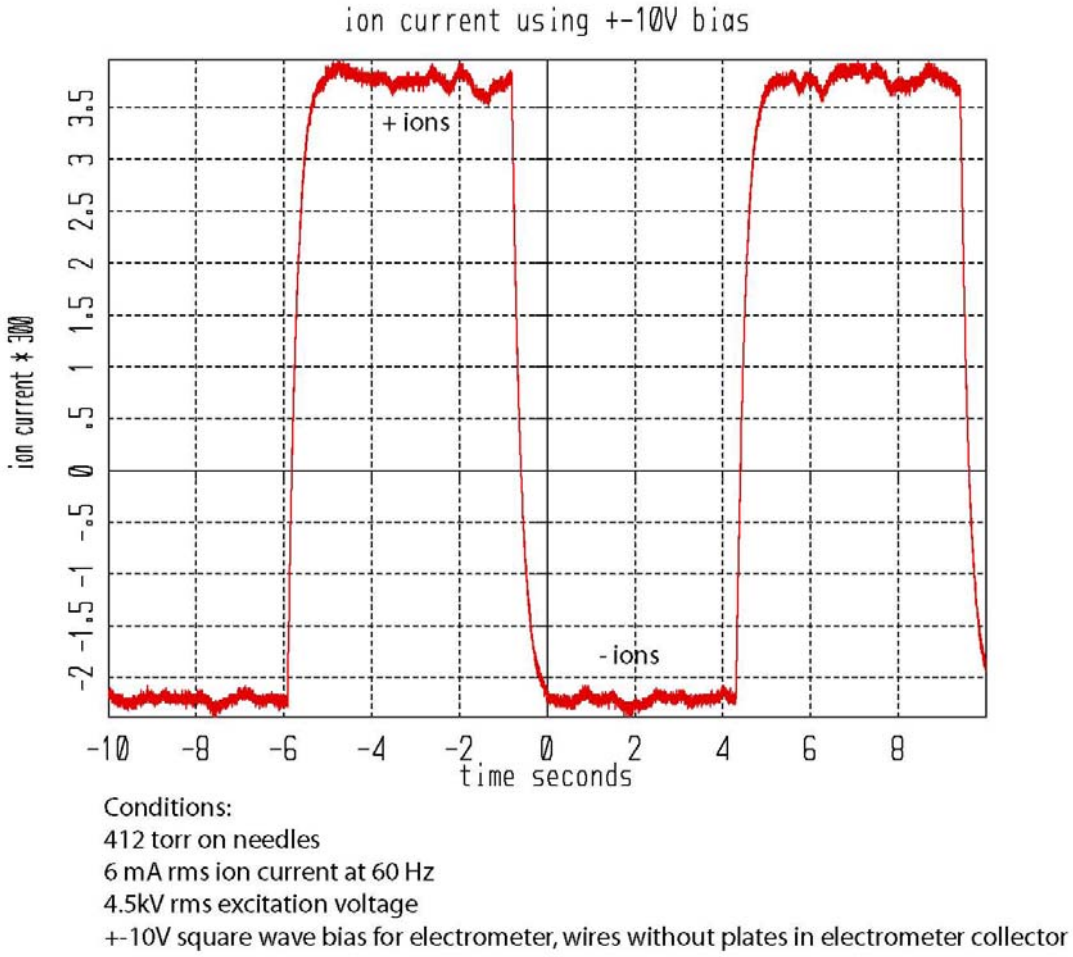

Figure 8 Ion currents measured by the sampling electrodes and electrometer in the gas flow after the apertures. The plasma flowing with the gas is neutral . The square wave polarizing voltage causes the charges to separate and flow to the electrometer sampling electrode as indicated in the schematic diagram **Figure 9**. A conjecture for the inequality of positive and negative ion currents is that the ionization dynamics at the needles causes N^+ ions to form on the positive cycle and N_2^- ions on the negative cycle.

As the AC excitation current increases, the sampling electrometer ion currents increase as well. The positive and negative ion currents remain close to equal. See **Figure 8**. The maximum ion current and best operating point occurs just below the excitation potential that causes a gas discharge. Typically, this occurs at 3kV rms, in agreement with the Paschen curve shown in **Figure 10** . When the discharge is excited the AC excitation current shows a discontinuous increase and the ion currents measured by the sampling electrometer changes character. The positive ion current increases by a factor of 4 to 5 while the negative ion current becomes small and is dominated by electrons. There is no mistaking when a discharge occurs. Once the discharge has been initiated the excitation voltage needs to be turned off and slowly increased again to just below the discharge voltage. If an oscilloscope is used to monitor the AC current the sampling point, the onset of a discharge can be seen to cause sharp spikes and 0.1MHz oscillations in the AC current (see **Figure 7**).

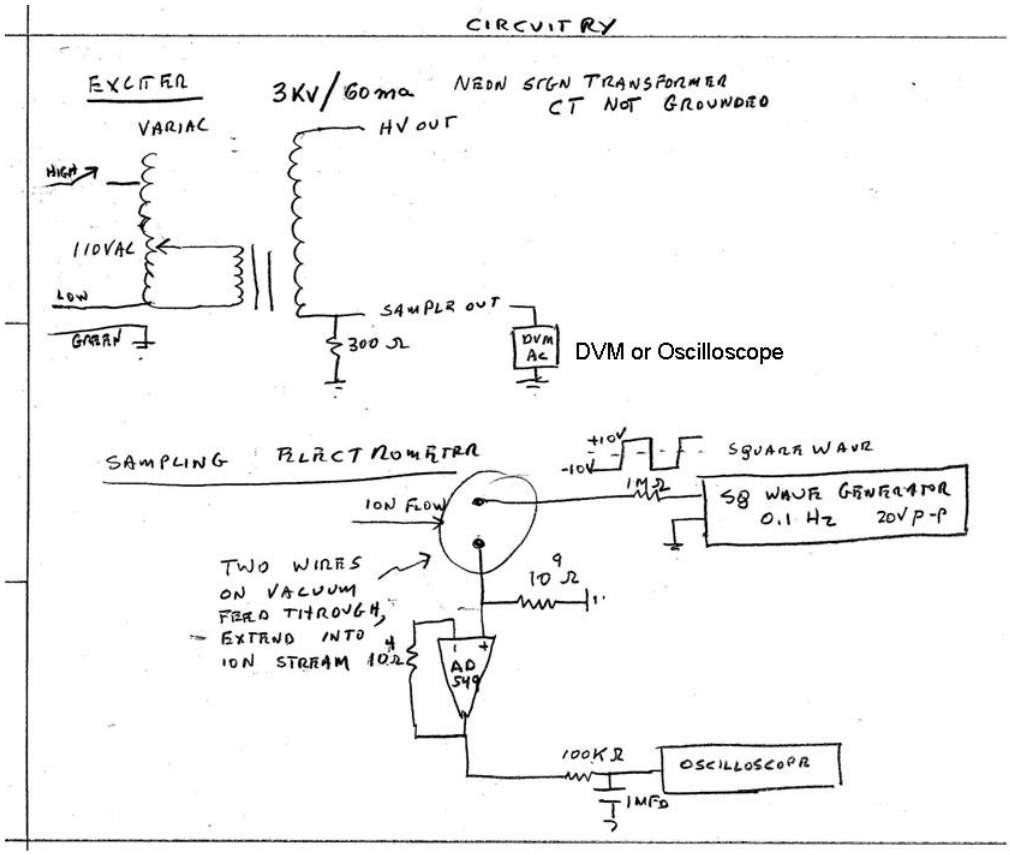

Figure 9 The exciter circuit, shown on the top, uses a Variac and a neon sign transformer. The transformer secondary needs to float relative to ground so that the AC current in the exciter can be measured at the 300 ohm sampling resistor. An oscilloscope is an effective means to look at the ionizing current. For small currents at low voltages before breakdown has been initiated and field ionization on the needle dominates, the waveform is close to sinusoidal. The onset of a discharge is noticed by a fast relaxation oscillation spike with ringing at about 50kHz. Once a discharge has been initiated, it takes several seconds with the voltage off to bring the system back to the field ionization corona state. The sampling electrometer circuit uses a pair of wires placed in the ion stream after the aperture. One wire collects the ions while the other produces a field to drive the ions to the collector.

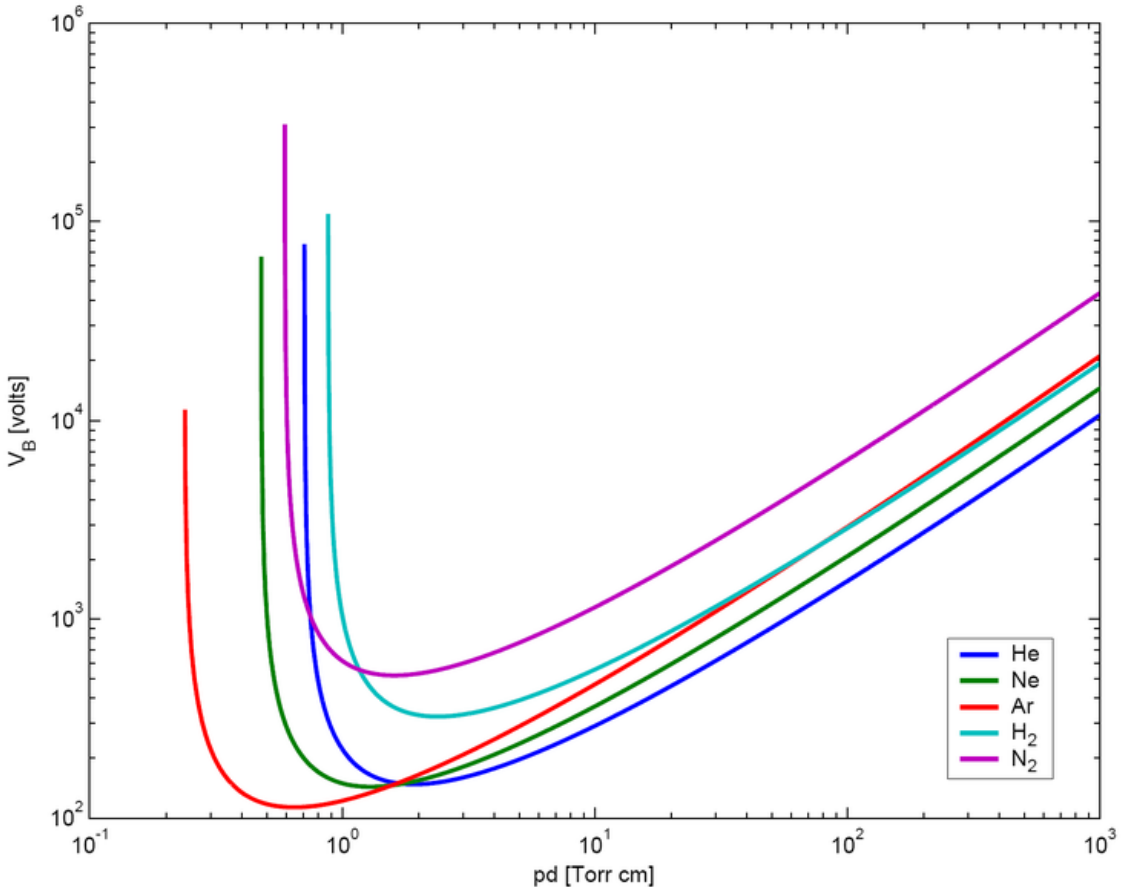

Figure 10 Paschen curves for different gases. The Paschen curve is the dividing line between corona and a gas discharge. For a given pressure and separation of the exciting electrodes, the curves provide the breakdown voltage initiating a gas discharge.

The LASTI Test

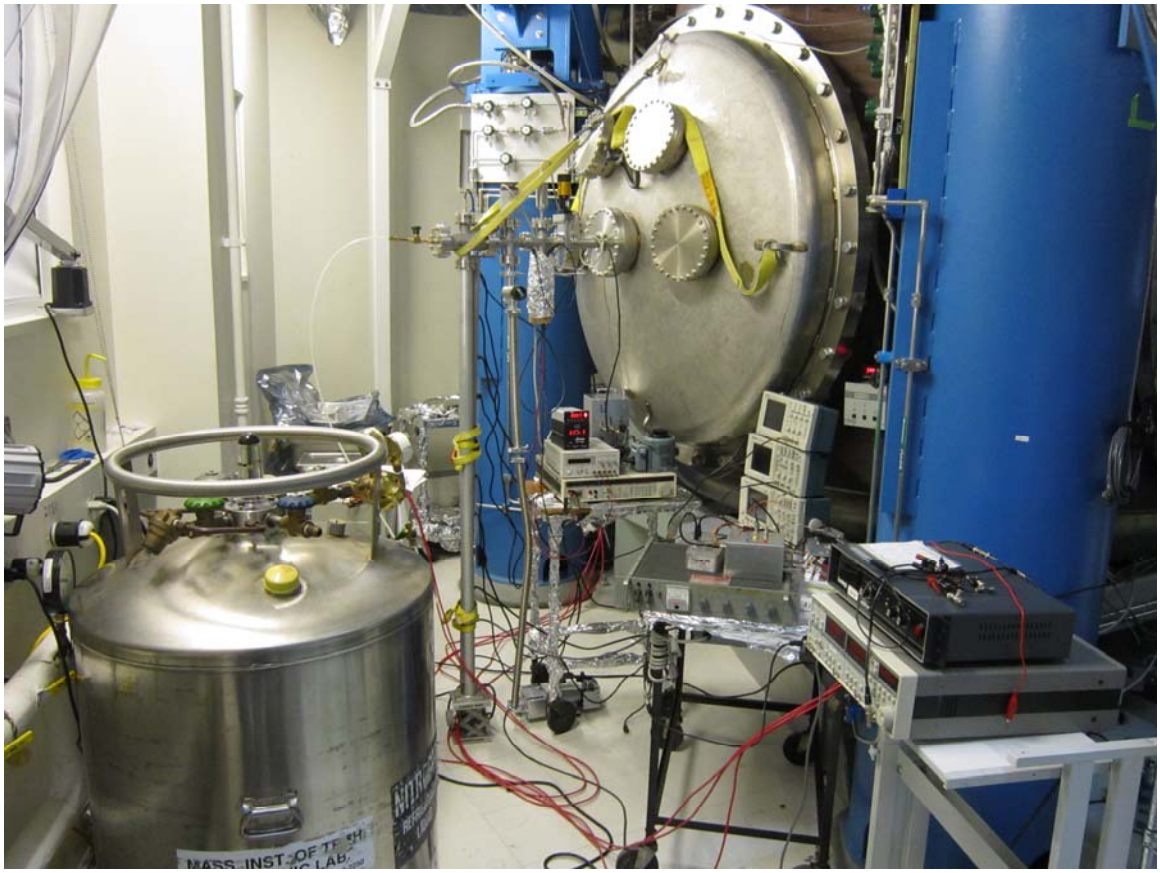

Figure 11 The LASTI test of charge neutralization. The boil off from the liquid nitrogen dewar on the left is used to provide the carrier gas. Charge was put on a full sized test mass by running a low current discharge between the electrodes of the electrostatic drive on the test mass. The charge was measured using the displacement associated with the electrostatic force on the test mass. The test mass was one mirror of an optical resonant cavity. **Figure 14** describes the method for separating the displacement from polarization forces and those due to a net charge.

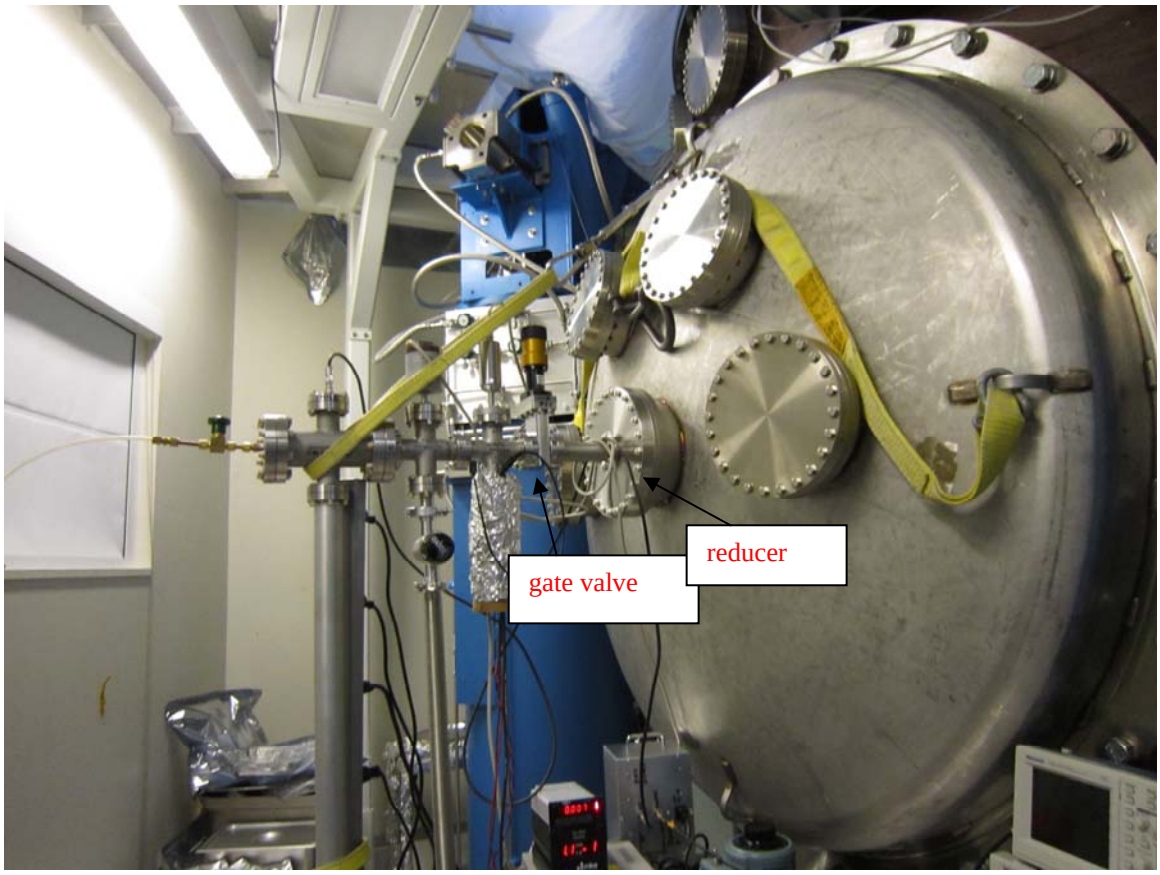

Figure 12 Close up of the installation. The gate valve, spool piece and zero length reducer from 10 inch CF to 2 ¾ CF needs to be mounted on each test mass chamber in LIGO to enable charge neutralization. Each LIGO site will have one plasma generator which is moved from chamber to chamber as needed.

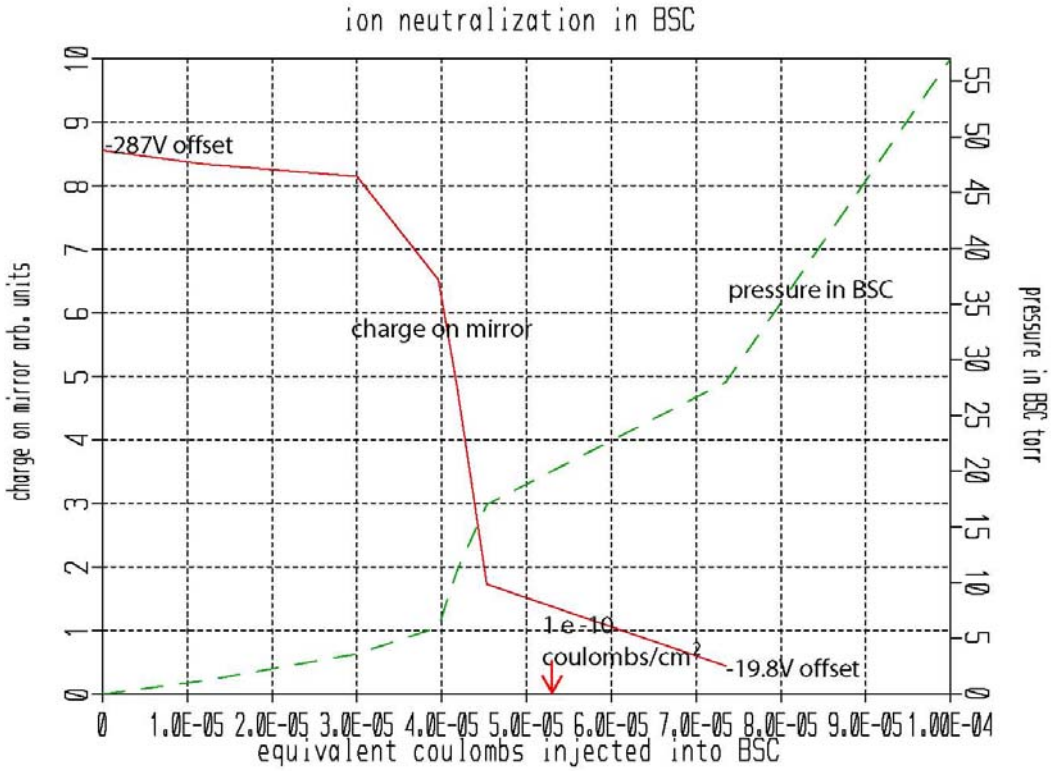

Figure 13 The results of the LASTI test. The red curve is a plot of the charge on the test mass as a function of the unipolar neutralizing ion charge injected into the system. The net charge injected is zero as positive and negative ion currents are about equal. The charge neutralization takes place by electric field driven diffusion of the ions in the neutral plasma near the test mass surface. The number density of free charges in the plasma stays close to the same throughout the injection but the field induced diffusion becomes smaller as the charge on the test mass becomes neutralized, leading to the observed exponential dependence of the charge remaining on the test mass. The pumps are turned off so the nitrogen pressure rises during the injection (the green curve). The x axis is an estimate of the unipolar charge that has flowed to all surfaces in the chamber from the plasma. The label -287Volt offset and -19.8 Volt offset are a measure of the charge remaining on the mirror by a test developed by John Miller of the Glasgow gravity group while he was resident at MIT.

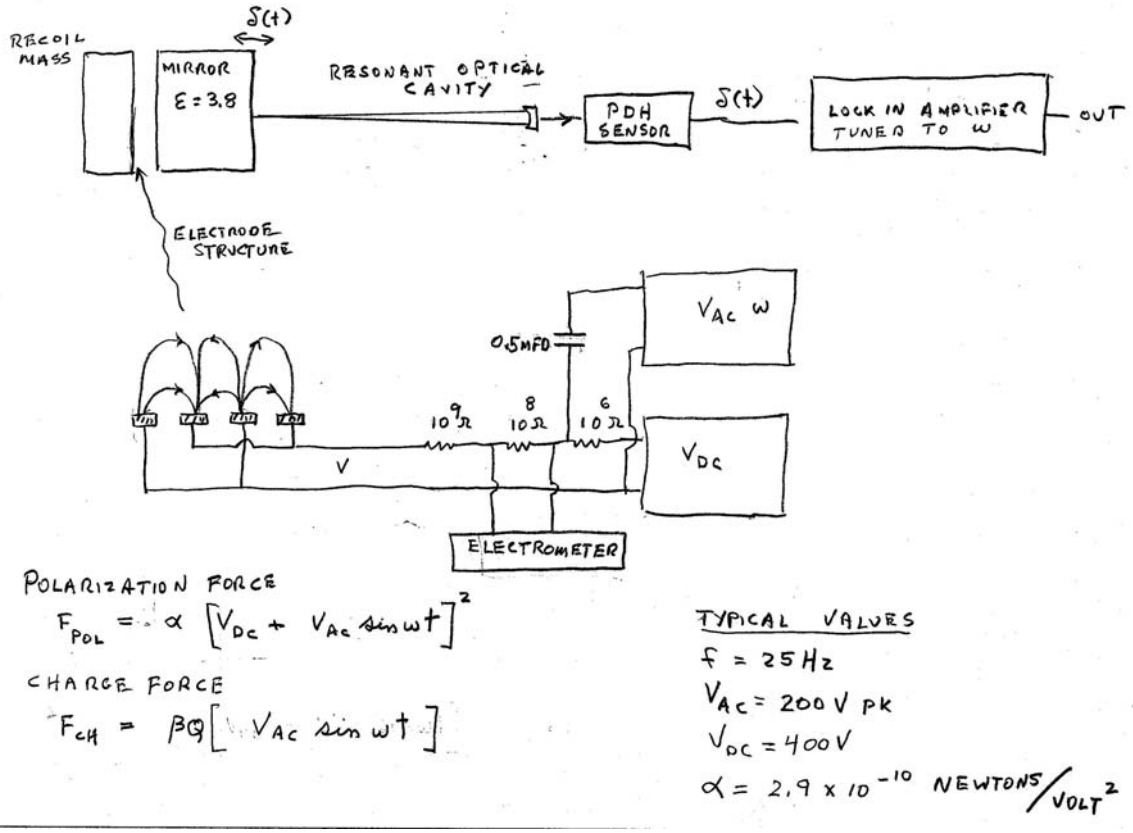

Figure 14 Method to measure the charge on the test mass. The force and displacement depend linearly on the charge on the test mass when the electrodes are driven by a voltage V_{AC}. For a sinusoidal drive at frequency f the displacement will be at f and directly measurable using a lock in amplifier to interrogate the control signal holding the cavity in lock. If there is no charge on the test mass the displacement depends on the square of the drive voltage providing only a 2f component in the control signal unless there is a bias voltage V_{DC} .

Test for damage to coated optical surface

To test whether damage is done to the coatings by the plasma and neutralization process, sample optically coated pieces were placed in the BSC. Control samples without the plasma and test samples with the plasma on were inserted. The control samples were placed in the BSC on April 12,13 at 0.1 torr. Test samples with the plasma were inserted on April 15,16. The chamber was at 0.18 torr before the plasma was injected with 2×10^{-8} ampere positive and negative ion current for ½ hour . The pressure on the Baratron gauge was 91 to 96 torr, while the pressure in the chamber varied from 0.18 to 19.5 torr . The Pirani gauge.pressure varied between 61 to 66 torr. The excitation voltage was between 2.4 to 2.6kV rms. The total single sign ion charge into chamber was 1/3 that of first test. The difference is that the LN2 tank had a lower efflux rate than the first tank.

Measurements made at Caltech show no change before and after exposure to the plasma in the HR coating absorption to the limit of the measurement which is about 0.2ppm loss.
There is also no change measured in the AR coatings but the data for these coatings is noisy with large fluctuations in the absorption with position on the surface both before and after exposure to the plasma. The measurements were performed by Liyuan Zhang (see **Appendix 2)**.

Appendix 1 Theoretical estimates

Some of the basic physics of the ion-generator is developed in this section. The principal result will be the estimate for the surface charge density on the mirror that can be neutralized by the product of the ion current injected into the main chamber and the exposure time.

The primary mechanism to generate ions occurs on the needles. I imagine the process as follows (proof will require more detailed work). During the time the needles are negative relative to ground, electrons are emitted by field emission from the needle points and some become attached to nitrogen molecules that flow by the needle tip to make negative ions. A small volume of the gas becomes momentarily negatively charged to close to the potential of the needle. During the positive part of the cycle, electrons are encouraged to make a transition from the nitrogen molecule into the metal of the needle by field enhanced tunneling. The missing electron causes the molecule to dissociate and leaves a positively charged atomic nitrogen ion in the gas stream. The potential of the charged region in the gas is close to that of the needle. The gas flowing past the needle tips becomes composed of sheets of positive and negative charge separated by a distance determined by the velocity of the gas past the needles times the ½ period of the 60Hz oscillation of the voltage – about 10^{-2} seconds. The gas rapidly becomes neutral as the positive and negative sheets inter-diffuse driven by the electric field between the sheets.

The mean free path of an ion placed in a neutral gas is $\lambda = \frac{1}{Q_{\text{ion-molecule}} \rho_{\text{\# molecules}}}$ where $Q_{\text{ion-molecule}}$ is the collision cross section of the ions with the neutral molecules and $\rho_{\text{\# molecules}}$ is the molecular number density. The ion – molecule cross section is about 40 times larger than the neutral - neutral crossection and is approximately 2 x10^{-14} cm^2. At 500 torr of molecular nitrogen, the mean free path of the nitrogen molecule ion is about 3 x 10^{-6} cm. The thermal velocity of the nitrogen molecule ion is $v_{th} = \sqrt{\frac{kT}{m_{ion}}}$ close to 3 x 10^4 cm/sec at room temperature. The thermal velocity and the mean free path give the diffusion constant for the ion in the gas, $D = 0.16\, v_{th} \lambda$. An ion initially trapped in the gas flow diffuses transverse to the flow in a time t by $s_{dif} = \sqrt{2\, D\, t}$. At 500 torr an ion will diffuse transverse to the main flow by about 0.5 mm in 0.1 seconds. The other means of transport is through the motion of the ion in response to electric fields. This mechanism is important in neutralizing the sheets of charge after the needles and also in neutralizing the charge on the surface of the mirror. A useful quantity is the mobility of the ion $\mu = \frac{v}{E} = \frac{e}{M_{ion}} < t > = \frac{e}{M_{ion}} \frac{\lambda}{v_{th}} \propto \frac{1}{\rho_{neutrals}}$ where v is the drift velocity of the ion limited by collisions with the neutral gas , E the driving electric field and M_{ion} the mass of the ion. At 500 torr the mobility of the nitrogen ion is about 2 cm/sec/volt/cm.

With an estimate of the gas velocity past the needles of 50 cm/sec and a potential of 2 kV between charge sheets, the neutralization time for the inter-diffusion of charge sheets is about 40 microseconds. The plasma has become neutral within 20 microns after it has left the needles.

Most of the ions formed at the needles are lost to recombination at the high charged particle (though neutral) densities between the needles and the apertures. The recombination rate depends on the product of the density of both types of charge carriers. The recombination rate at atmospheric pressure is given in units of number/cm^3/sec, $R_{recom} \sim 1 \times 10^{-6} \rightarrow 1 \times 10^{-7} n^2$ where n is the number of ions/cm^3 . The flow spends about 10 milliseconds between the needles and apertures giving a maximum ion density surviving recombination between 10^8 to 10^9 ions/cm^3 . After the apertures the ion density is reduced sufficiently for diffusion to the wall to dominate the ion loss. Inside the apertures the flow is turbulent and the ions pass through the aperture with little loss, a fact not known at the outset of the research.

The ion flow I_{ion} into the chamber is measured with the sampling electrometer system directly, typically being the equivalent of 3×10^{-8} amperes (about 2×10^{11} ions/sec) of both sign. Once the ions make it into the chamber, they distribute uniformly throughout the volume entrapped in the neutral gas. Assume the total area of the chamber and other surfaces exposed to the gas in the chamber is A. The ion flow to the surface is able to neutralize a surface charge density $\sigma = \frac{I_{ion} t}{A}$ where t is the filling time in seconds . Using the surface of a BSC chamber A = 6×10^5 cm^2 and a filling time of 1 hour, the surface charge on the mirror that can be neutralized is about 2×10^{-10} coulombs/cm^2 .

The volume of the BSC chamber is approximately 3×10^7 cc. During the initial filling process the ion density grows linearly at a rate of about 10^4 ions/cc/sec and then levels off at equilibrium when the losses to the walls are made up by the input plasma flow.

The neutralization actually goes a little more quickly than the prior estimate as the diffusion to the charged surface is driven by the field from the surface charge. The volume from which ions are drawn to neutralize the surface is roughly the sphere determined by the Debye screening length $\lambda_D = \sqrt{\frac{kT}{4\pi n e^2}}$ = 2 cm for the conditions in the BSC tank (using cgs units: e = 4.8×10^{-10} esu, n = 2×10^3 ions/cc, k = the Boltzmann constant and T = 300K).

The electric field in the plasma around the charged surface patch on the mirror can be approximated as $E = \frac{Q e^{-\lambda r}}{r^2}$ where Q is the charge on the surface and r the distance from the surface. The neutralizing current drawn to the surface is estimated by integrating the flow to the surface using the ion mobility μ. The charge remaining on the patch with time is given by $Q(t) = Q e^{-\frac{4\pi e n(t) \mu t}{\lambda_D(t)}}$. The time dependence of the Debye length and the ion density is to account for the time to establish an equilibrium ion density set by the diffusion to the surface and the input ion current during the initial filling of the chamber. With the estimated parameters from above, the time constant at equilibrium is about 500 seconds. A further refinement is needed to account for the change in ion density as the chamber is filled with the plasma. The filling slows the process down giving an overall $t^{\frac{5}{2}}$ initial time dependence in the exponential. The flattening at small times is seen in the experimental data (**Figure 13**) as the chamber fills.

Some discussion of the experiment and theory

What is known for sure about the ions? The mechanism at the needles is a guess. Much of the uncertainty would be settled by using a mass spectrometer in the ion flow. One worry was that the ionization was due to gas impurity in the flow such as Oxygen or Argon. Both were tried directly and led to different results. Another worry was that the negative ions were really electrons. The hypothesis was tested with magnetic fields from permanent magnets along the flow and no changes were observed in the positive and negative ion currents in the sampling electrometer. Once a discharge has been ignited, the negative charge carriers are electrons and are influenced by magnetic fields.

Another thought was that the negative currents were due to photoeffect electrons from UV generated by recombination near the needles, most likely not the case as the ion flow measured in the sampling electrometer depends almost linearly on the neutral carrier gas velocity.

Appendix 2 Results from the optical absorption tests on samples before and after exposure to the plasma as well as after exposure to the residual gas in the LASTI BSC without a plasma.

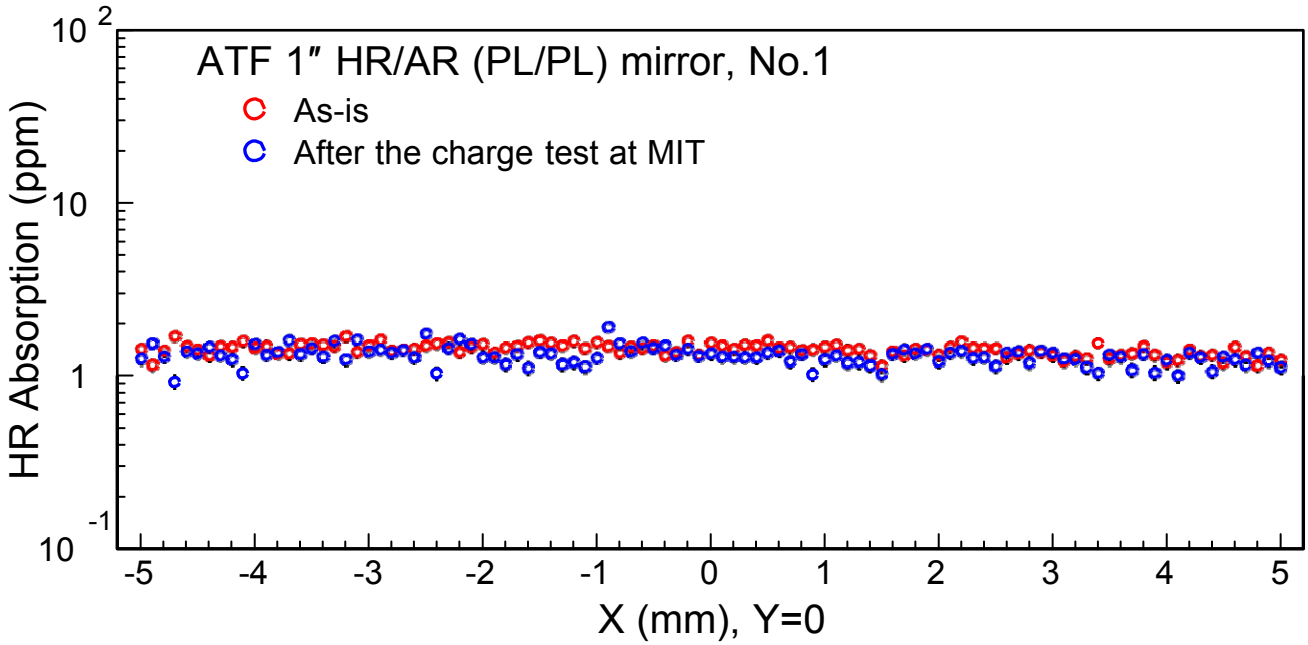

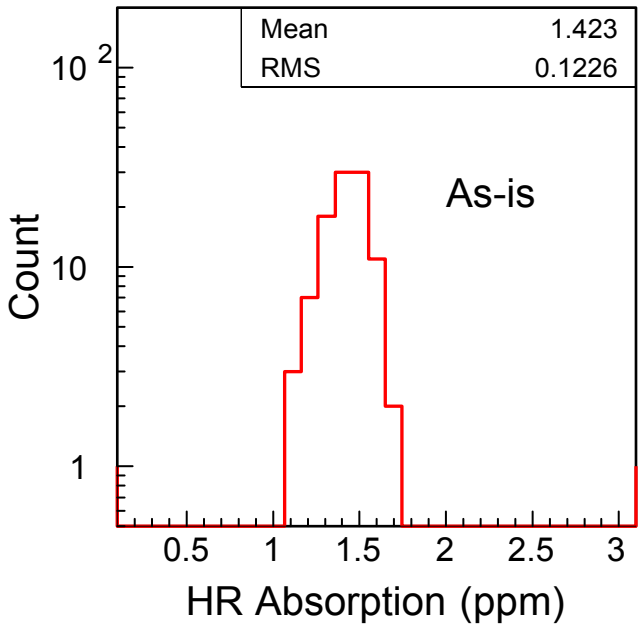

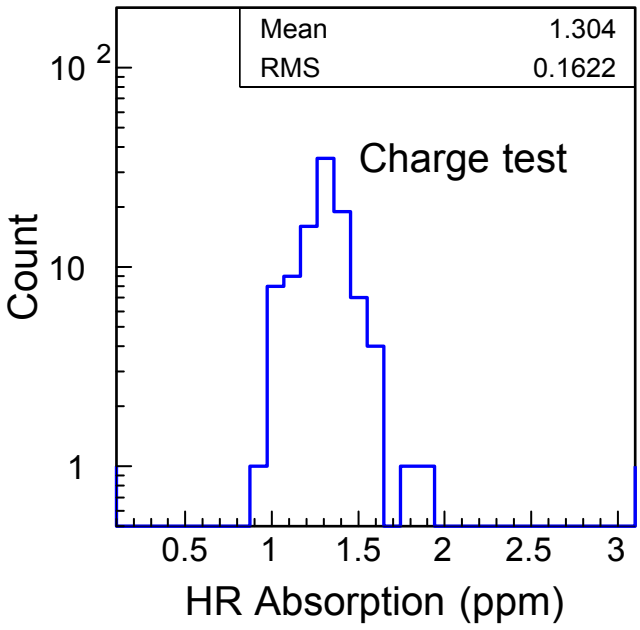

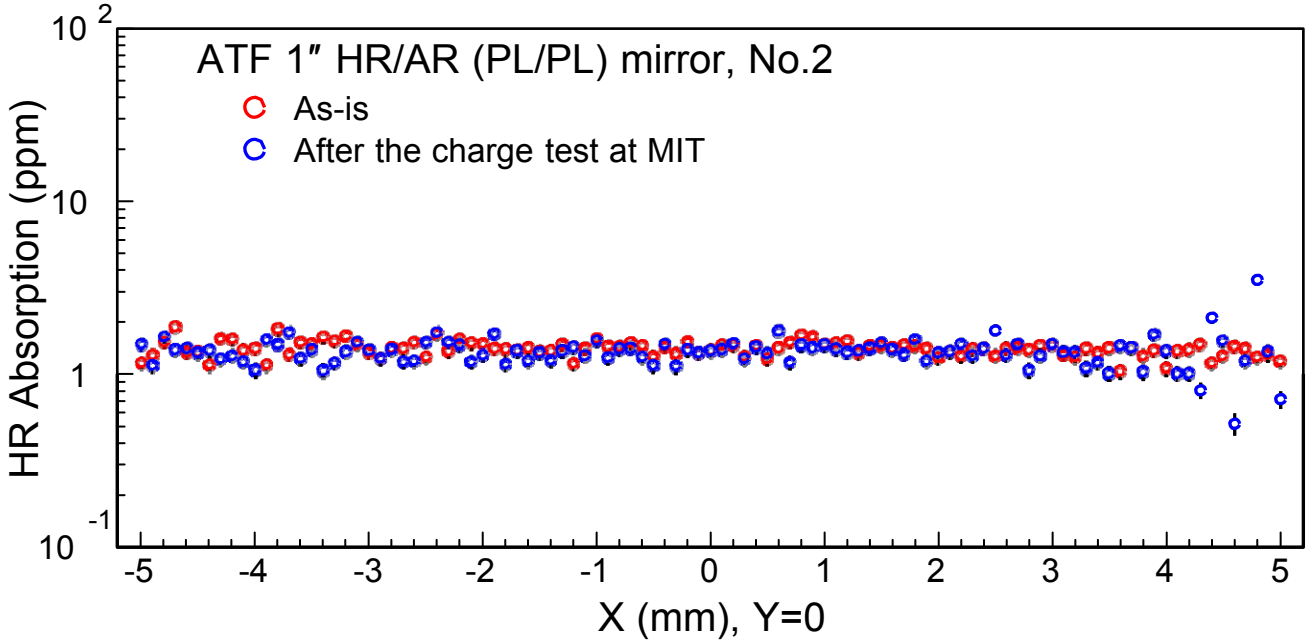
ATF 1″ HR/AR (PL/PL) mirror, No.2
As-is
After the charge test at MIT
HR Absorption (ppm)
X (mm), Y=0

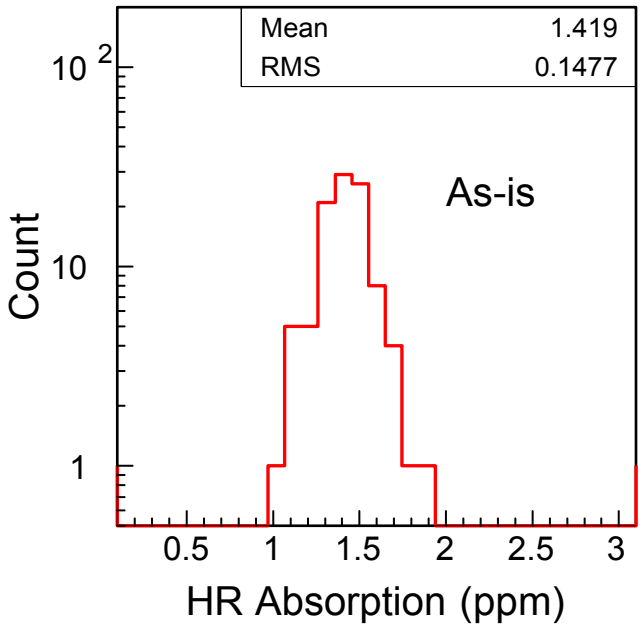
Mean 1.419
RMS 0.1477
As-is
Count
HR Absorption (ppm)

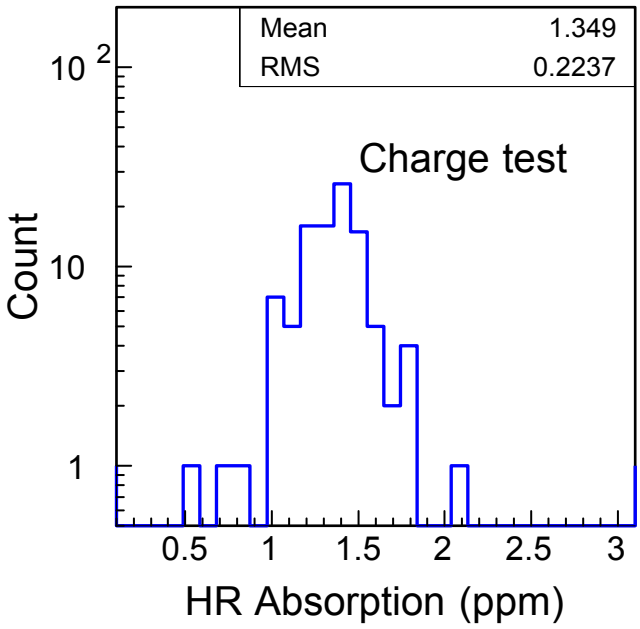
Mean 1.349
RMS 0.2237
Charge test
Count
HR Absorption (ppm)

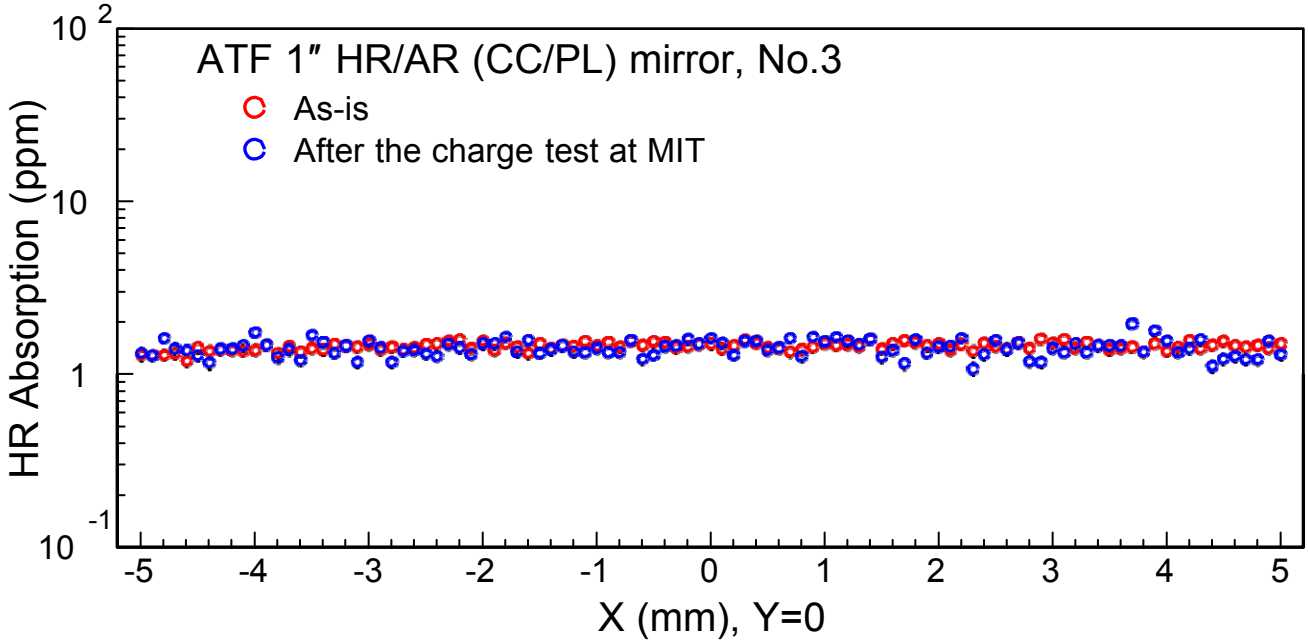
ATF 1″ HR/AR (CC/PL) mirror, No.3
As-is
After the charge test at MIT
HR Absorption (ppm)
X (mm), Y=0

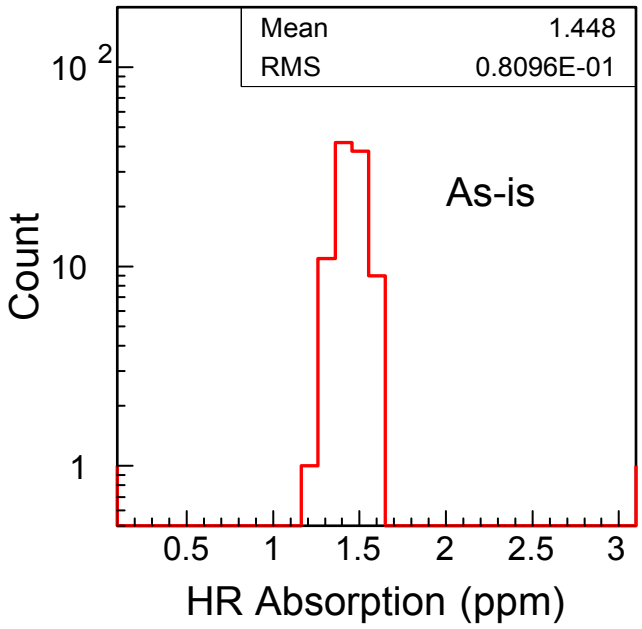
Mean 1.448
RMS 0.8096E-01
As-is
Count
HR Absorption (ppm)

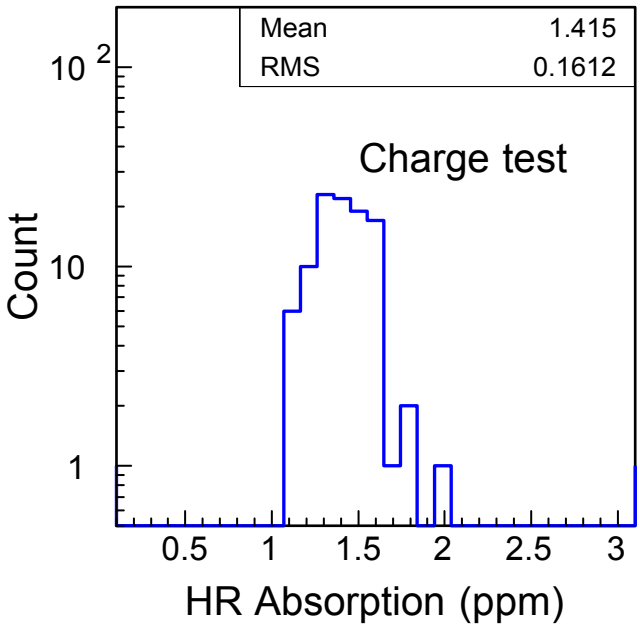
Mean 1.415
RMS 0.1612
Charge test
Count
HR Absorption (ppm)

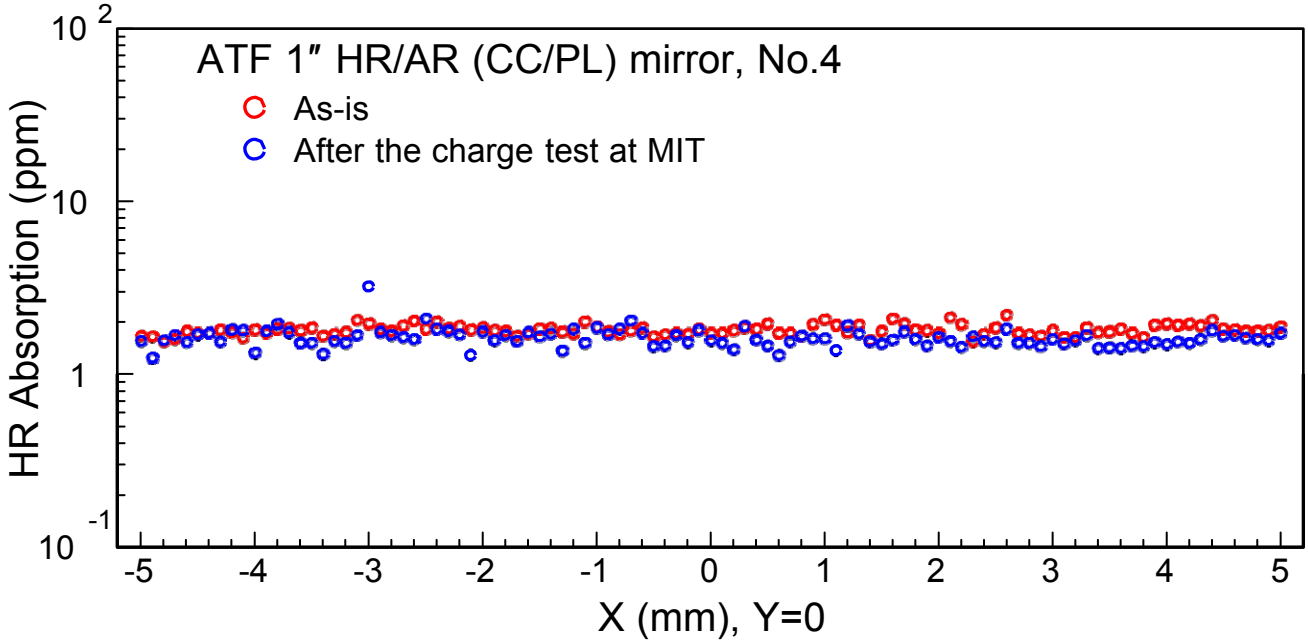
ATF 1″ HR/AR (CC/PL) mirror, No.4
As-is
After the charge test at MIT
HR Absorption (ppm)
X (mm), Y=0

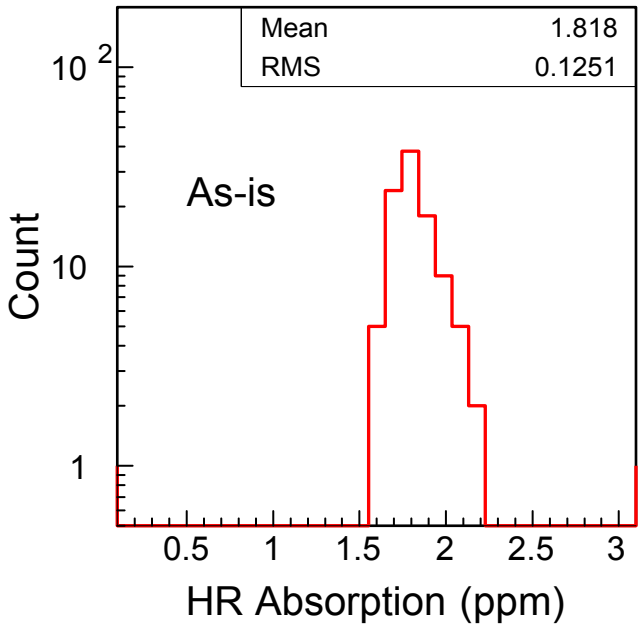
Mean 1.818
RMS 0.1251
As-is
Count
HR Absorption (ppm)

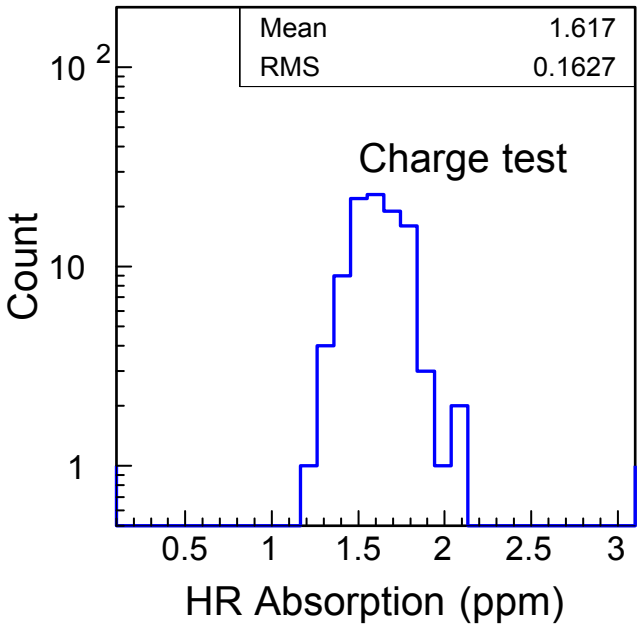
Mean 1.617
RMS 0.1627
Charge test
Count
HR Absorption (ppm)

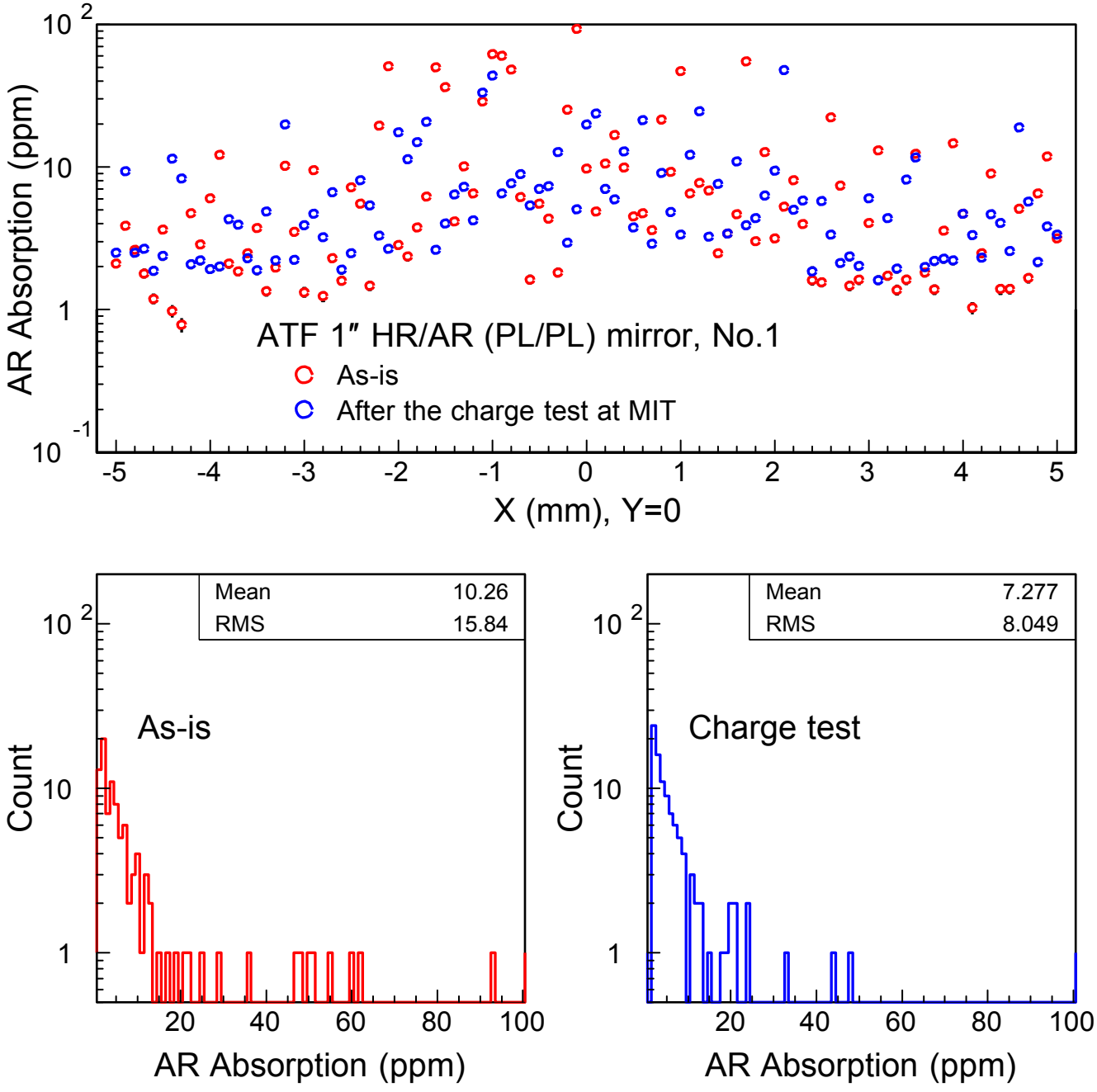
AR Absorption (ppm)
X (mm), Y=0
ATF 1″ HR/AR (PL/PL) mirror, No.1
As-is
After the charge test at MIT
Mean 10.26
RMS 15.84
As-is
Count
AR Absorption (ppm)
Mean 7.277
RMS 8.049
Charge test
Count
AR Absorption (ppm)

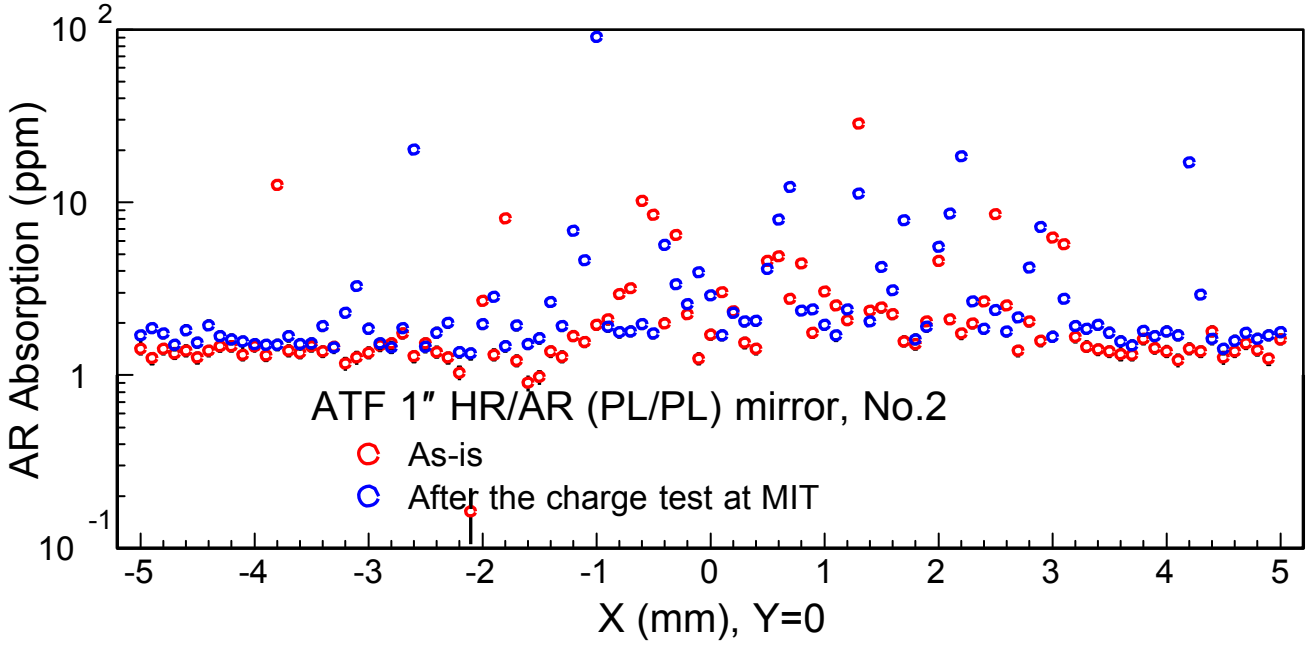
AR Absorption (ppm)
X (mm), Y=0
ATF 1″ HR/AR (PL/PL) mirror, No.2
As-is
After the charge test at MIT

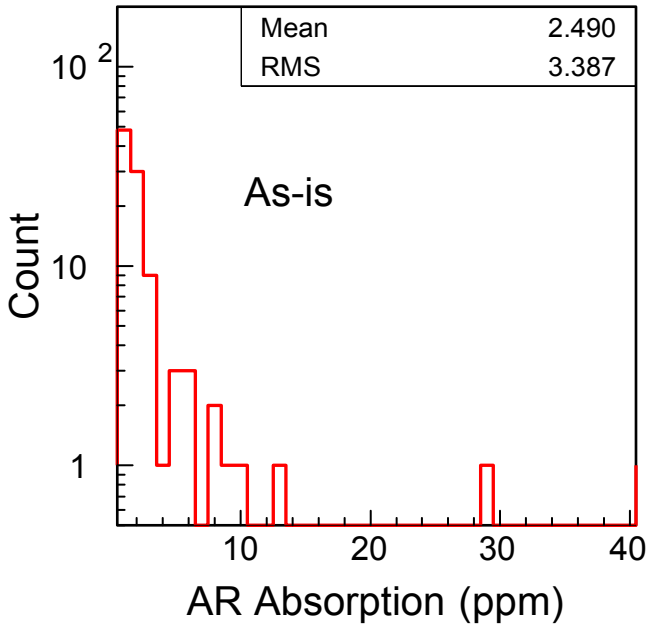
Mean 2.490
RMS 3.387
As-is
Count
AR Absorption (ppm)

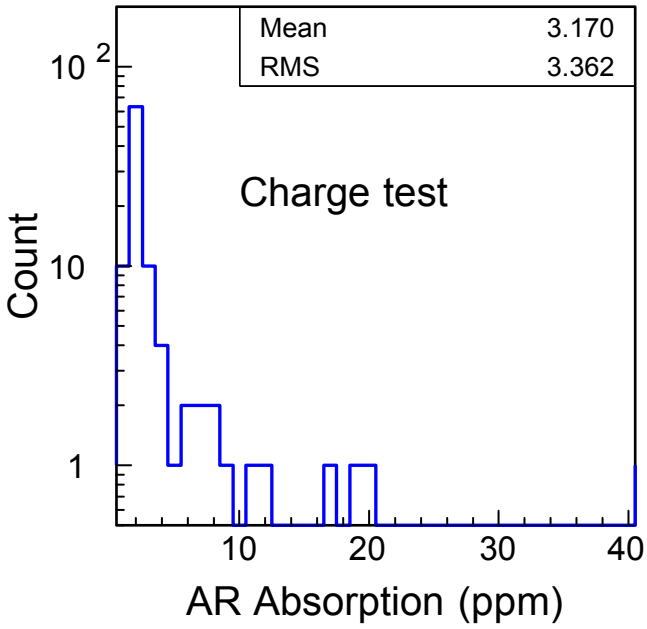
Mean 3.170
RMS 3.362
Charge test
Count
AR Absorption (ppm)

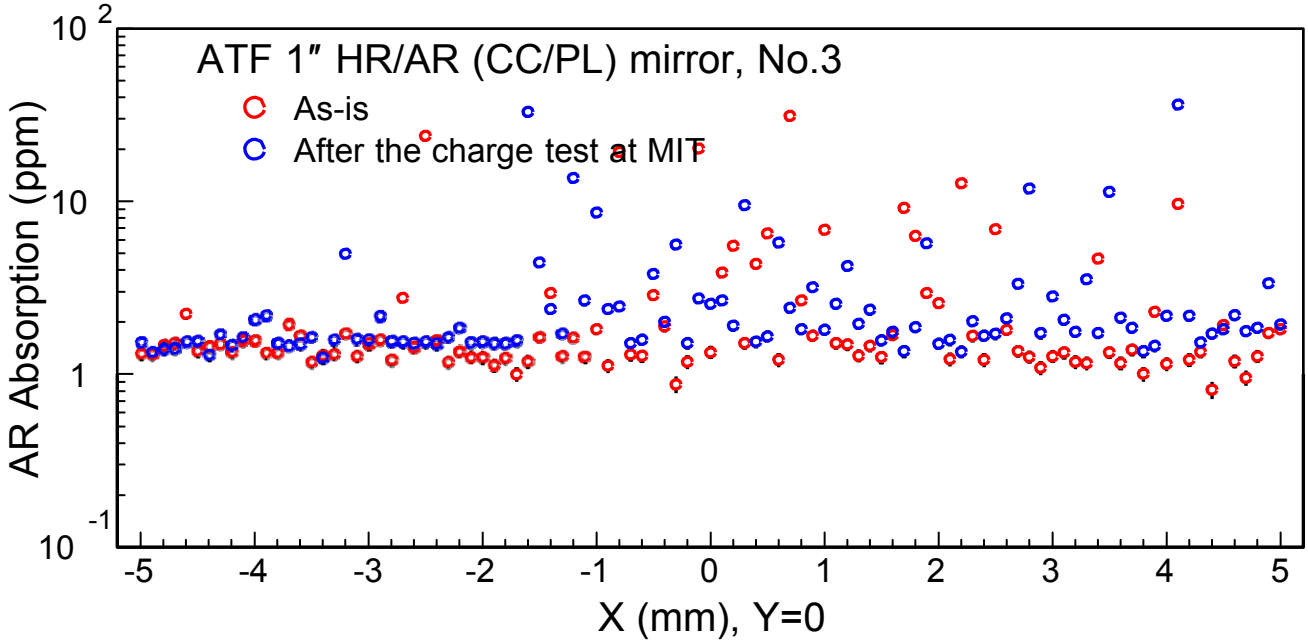
ATF 1″ HR/AR (CC/PL) mirror, No.3
As-is
After the charge test at MIT
AR Absorption (ppm)
X (mm), Y=0

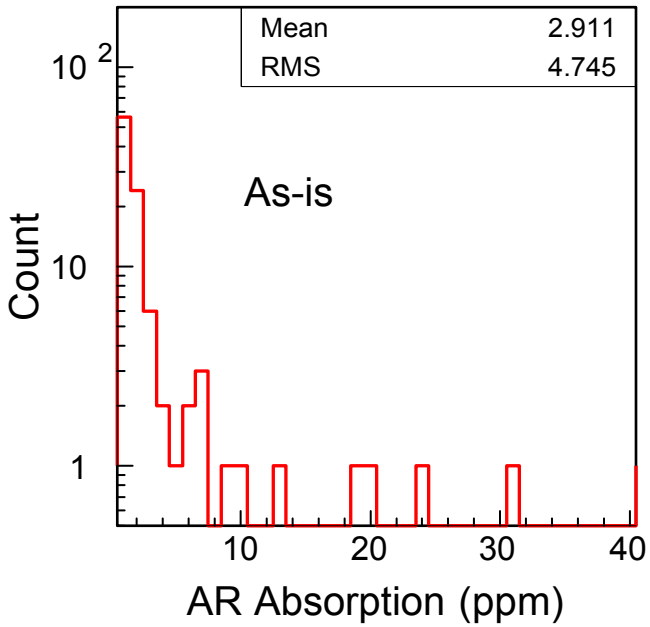
Mean 2.911
RMS 4.745
As-is
Count
AR Absorption (ppm)

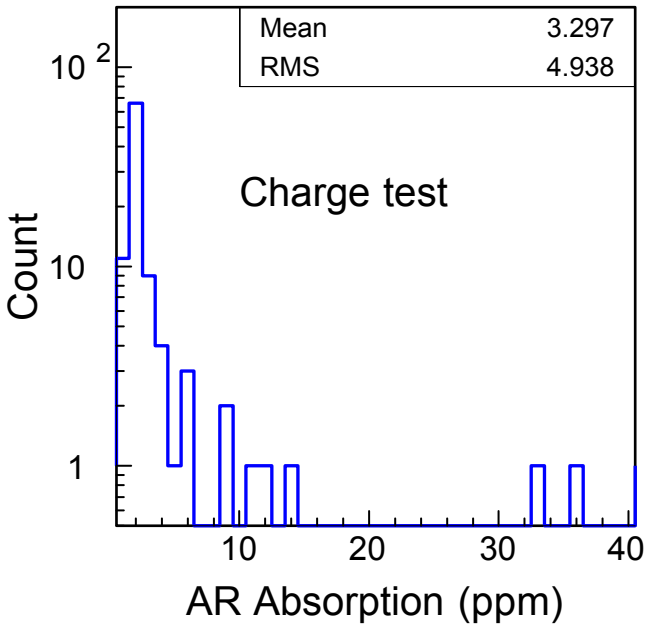
Mean 3.297
RMS 4.938
Charge test
Count
AR Absorption (ppm)

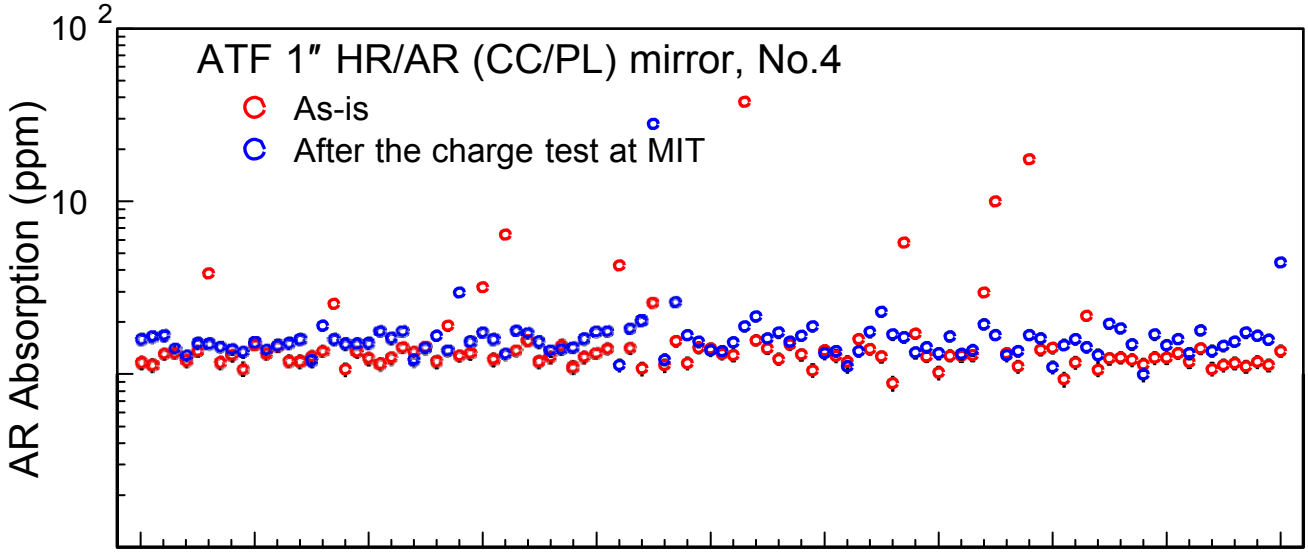
ATF 1″ HR/AR (CC/PL) mirror, No.4
As-is
After the charge test at MIT
AR Absorption (ppm)
10 2
10

Appendix 3 Detail drawings and parts list

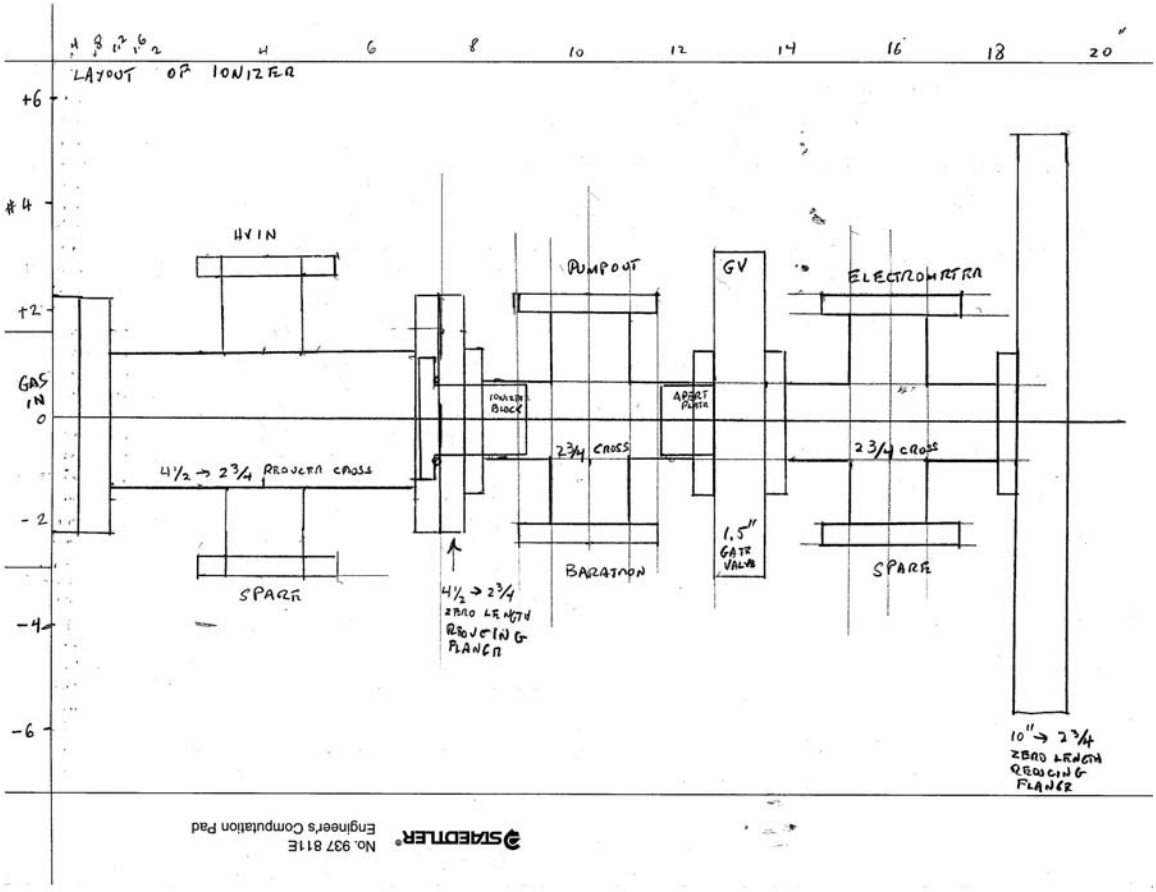

Figure 1 app3: Detailed layout of the ionizer. Final version has the electrometer cross and the gate valve interchanged. The spare flange on the electrometer cross holds a Pirani gauge. In order to use the "zero" length adapter from 2 ½ inch to 10 inch conflat, a 2 ½ inch conflat spool piece is required between the gate valve and the adapter.

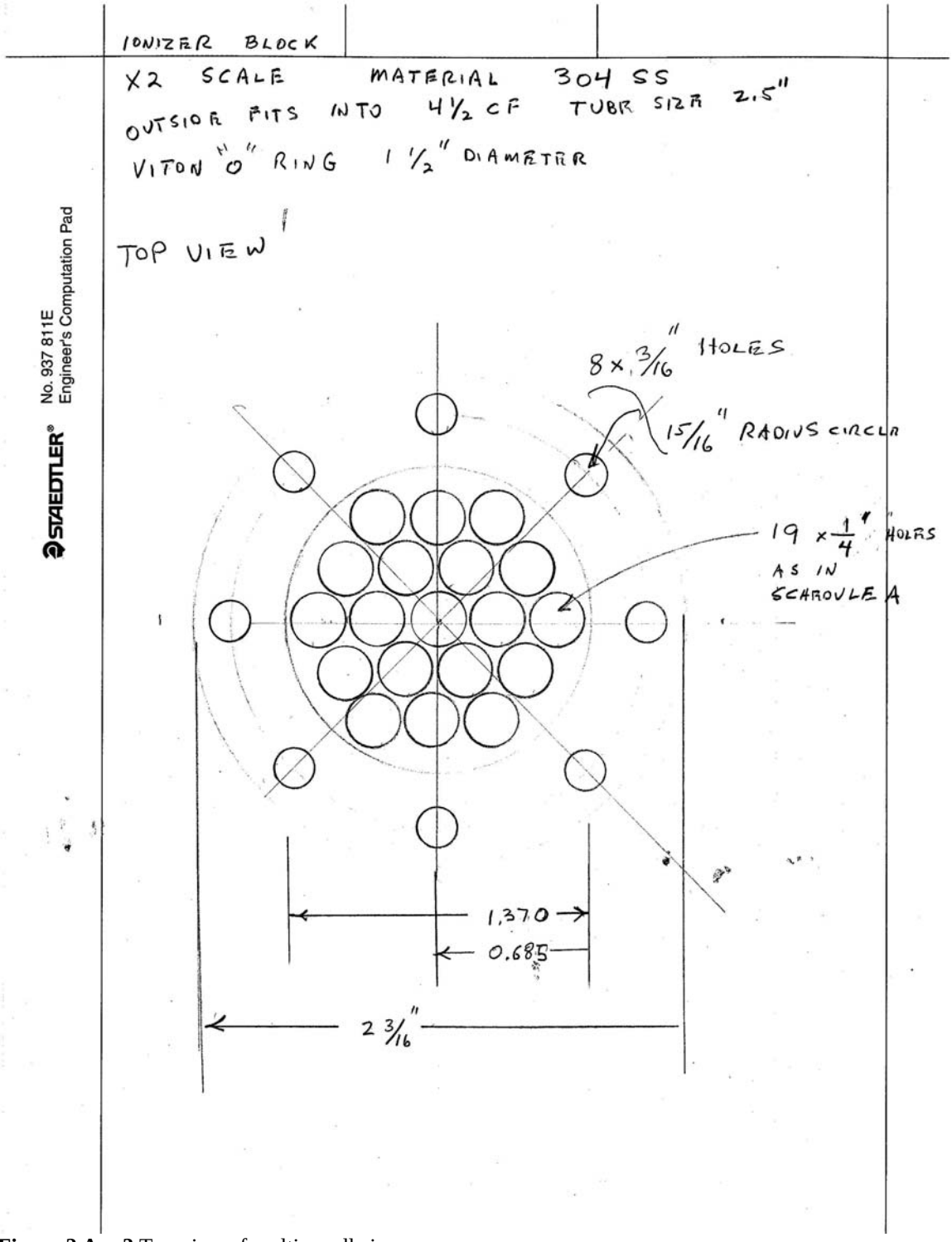

Figure 2 App3 Top view of multi-needle ion source.

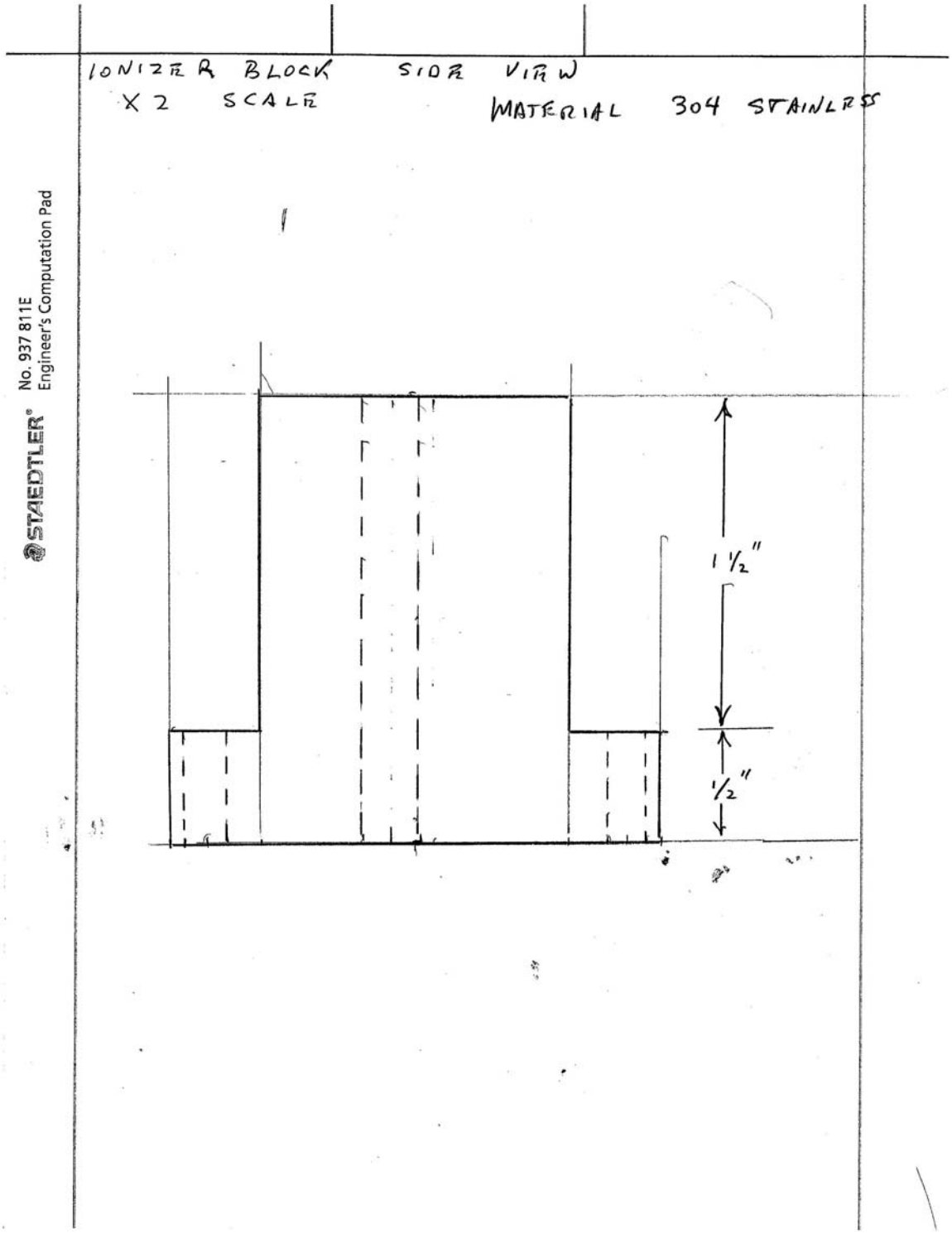

Figure 3 App3 Side view of multi-needle ion source.

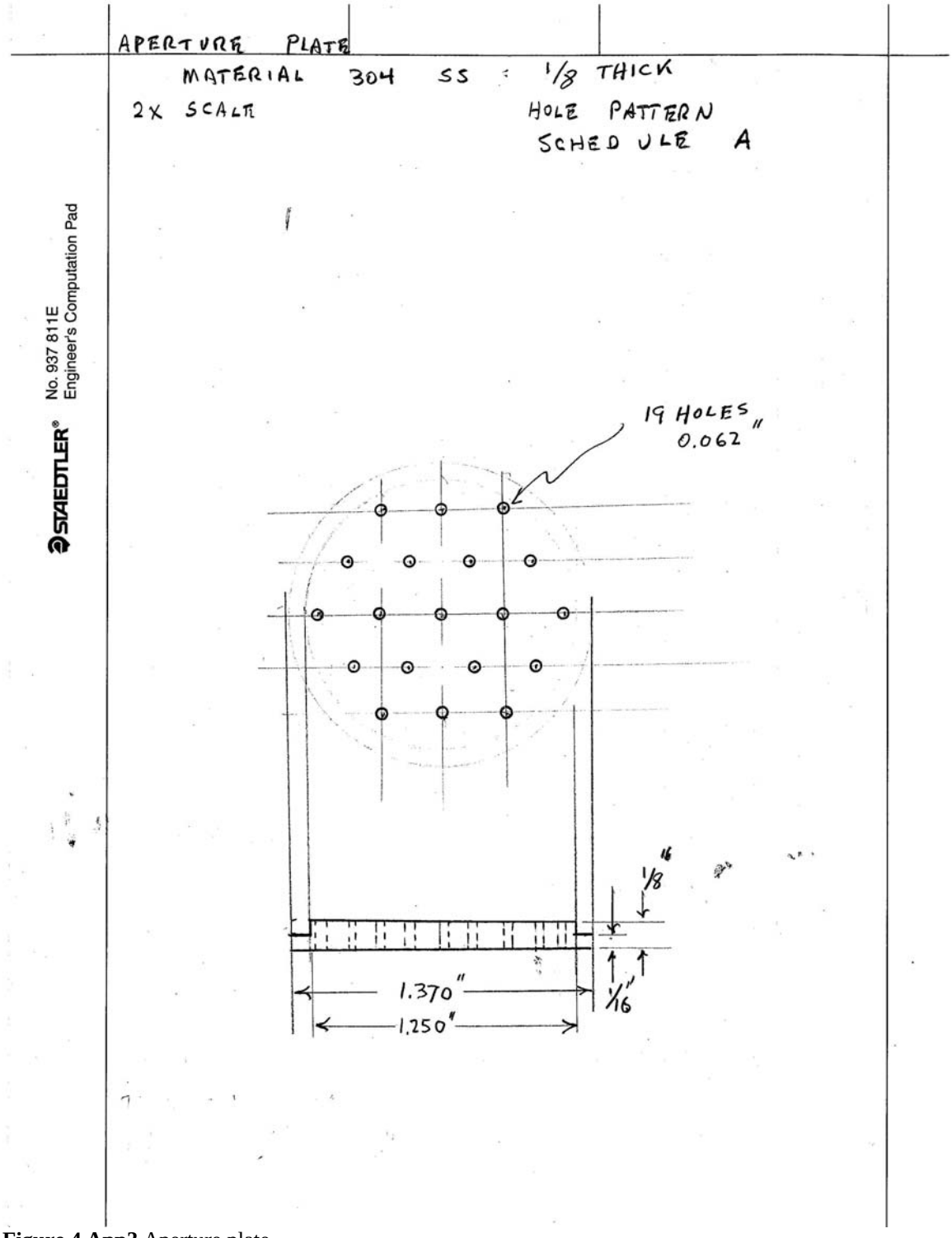

Figure 4 App3 Aperture plate.

schedule_A_hole_pattern.txt

schedule A hole pattern

hole #	x	y
1	0.000	0.0000
2	0.2750	0.0000
3	0.5500	0.0000
4	-.2750	0.0000
5	-.5500	0.0000
6	0.1375	0.2382
7	0.4125	0.2382
8	-.1375	0.2382
9	-.4125	0.2382
10	0.0000	0.4764
11	0.2750	0.4764
12	-.2750	0.4764
13	0.1375	-.2382
14	0.4125	-.2382
15	-.1375	-.2382
16	-.4125	-.2382
17	0.0000	-.4764
18	0.2750	-.4764
19	-.2750	-.4764

Table 1 App3 ¼ inch hole location in the multi-needle ion source block in inches. Center of block is x=0, y=0.

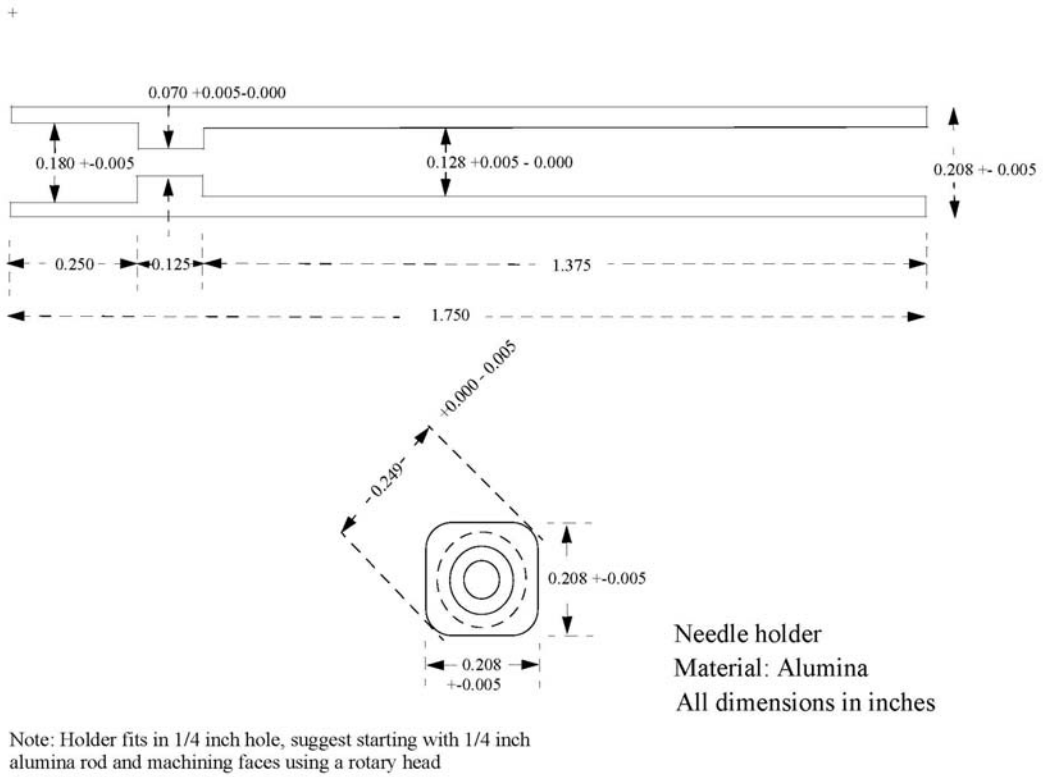

Figure 5 App3 Detail of the alumina needle holders.

Purchases for ion generator to be mounted on LASTI flange to neutralize charge on mirror

Vacuum equipment to be purchased from MDC

description	quantity	MDC number	cost/item	cost
4 1/2 CF blank flange	1	110018	53.00	53.00
2 3/4 CF blank flange	3	110008	15.00	45.00
4 1/2 to 2 3/4 reducer	1	150008	94.00	94.00
10 to 2 3/4 reducer	1	150037	259.00	259.00
4 1/2 to 2 3/4 reduce cross	1	405041	396.00	396.00
2 3/4 cross	2	405002	121.00	242.00
2 3/4 half nipple	1	401002	34.00	34.00
2 3/4 20 pin feedthru	1	647052	435.00	435.00
2 3/4 2 pin MHV feedthru	1	632002	135.00	135.00
2 3/4 manual gate valve viton	1	300001	1118.00	1118.00

Vacuum equipment to be purchased from MKS instruments

baratron gauge 2 3/4 conflat	1	model 622B13TLE	1049.00
readout and power supply	1	model 660B	
pirani gauge 2 3/4 conflat	1	model 103450014	228.00
gauge controller	1	model 945-A-120-TR	514.00
cable for pirani gauge	1	model 10317000654	64.00

Needle holder insulators Material Alumina

T.Q. Abrasive Machining, Inc	20	Initial 20 pieces	$30/piece

Parts to be bought from Vishay - Dale

5W 4megohm cermet film resistors	50	HVW002 series